ISTANBUL TECHNICAL UNIVERSITY ★ GRADUATE SCHOOL OF SCIENCE ENGINEERING AND TECHNOLOGY

LONGITUDINAL DISPERSION OF HEAVY PARTICLES IN A FREE SURFACE FLOW OVER ROUGH BED

M.Sc. THESIS

Selçuk DEMİRBAŞ

Coastal Sciences And Engineering Department

Coastal Sciences And Engineering Programme

JUNE 2015

ISTANBUL TECHNICAL UNIVERSITY ★ GRADUATE SCHOOL OF SCIENCE ENGINEERING AND TECHNOLOGY

LONGITUDINAL DISPERSION OF HEAVY PARTICLES IN A FREE SURFACE FLOW OVER ROUGH BED

M.Sc. THESIS

Selçuk DEMİRBAŞ
(517091013)

Coastal Sciences And Engineering Department

Coastal Sciences And Engineering Programme

Thesis Advisors:
Assoc. Prof. Dr. V. Ş. Özgür KIRCA
Prof. Dr. Sedat KABDAŞLI

JUNE 2015

<u>**İSTANBUL TEKNİK ÜNİVERSİTESİ ★ FEN BİLİMLERİ ENSTİTÜSÜ**</u>

SERBEST YÜZEY AKIMINDA PÜRÜZLÜ TABAN ÜZERİNDE AĞIR PARÇACIKLARIN BOYUNA DİSPERSİYONU

YÜKSEK LİSANS TEZİ

Selçuk DEMİRBAŞ
(517091013)

Kıyı Bilimleri Ve Mühendisliği Anabilim Dalı

Kıyı Bilimleri Ve Mühendisliği Programı

Tez Danışmanları:
Doç. Dr. V. Ş. Özgür KIRCA
Prof. Dr. Sedat KABDAŞLI

HAZİRAN 2015

Selçuk DEMİRBAŞ, a **M.Sc.** student of ITU **Graduate School Of Science, Engineering And Technology** student ID **517091013**, successfully defended the **thesis** entitled "**LONGITUDINAL DISPERSION OF HEAVY PARTICLES IN A FREE SURFACE FLOW OVER ROUGH BED**", which he prepared after fulfilling the requirements specified in the associated legislations, before the jury whose signatures are below.

Thesis Advisor :	**Prof. Dr. Sedat KABDAŞLI** Istanbul Technical University	....
Co-advisor :	**Assoc. Prof. Dr. V. Ş. Özgür KIRCA** Istanbul Technical University	....
Jury Members :	**Prof. Dr. Hafzullah AKSOY** Istanbul Technical University	....
	Asst. Prof. Dr. Ahmet Ozan ÇELİK Anadolu University	....
	Asst. Prof. Dr. Burak AYDOĞAN Yıldız Technical University	....

Date of Submission : 04 May 2015
Date of Defense : 02 Jun 2015

To my dear family,

FOREWORD

Turbulence is a natural phenomenon, science is yet to explain. This study will introduce a numerical model to inspect turbulent dispersion, an important result of turbulence, under the effect of bed roughness, using the random walk technique

I wish to express my gratitude to Assoc. Prof. Dr. V. Ş. Özgür Kırca, for everything he has taught me, his endless patience, brotherly guidance and trust. Every word he said was an inspiration itself.

I also wish to thank Prof. Dr. Sedat Kabdaşlı for giving me the opportunity to work on such a great topic with such great people, and guiding me in and through the M.Sc. programme.

I'm also grateful to my wife, whom I met at the start of this programme, and is the mother of my dear son right now.

May 2015 Selçuk DEMİRBAŞ

TABLE OF CONTENTS

Page

ABBREVIATIONS

A	: Cross-sectional Flow Area of Main Channel
A_S	: Cross-sectional Area of TS Zone
A_d	: Damping Coefficient
β	: Rouse Parameter
$\bar{c}$	: Time-averaged Concentraton
C	: Solute Concentration in Main Channel
C_S	: Solute Concentration in Storage Zones
< c >	: Cross-sectional Average Concentration
D_1	: Diffusion Coefficient
D	: Dispersion Coefficient
DNS	: Direct Numerical Simulation
h	: Flow Depth
k_s^+	: Roughness Reynolds Number
k_s	: Equivalent Sand Roughness
κ	: Von Karman Constant
K_S	: Longitudinal Dispersion Coefficient Excluding The TS Effect
l_p	: Penetration Length Scale
L	: Flow Characteristic Scale
LES	: Large Eddy Simulation
N	: Number of Particles
Π	: Wake Strength Parameter
Re	: Reynolds Number
Re_f	: Friction Reynolds Number
δ_b	: Boundary Near Bed
T_1	: Mean Bursting Period
TS	: Transient Storage
T_C	: Main Residence Time Of Solute in Storage Zones
T	: Nondimentional Time
t	: Time
τ_0	: Bed Shear Stress
t_0	: Arbitrary Time
u’	: Velocity Fluctiation at x Direction
U	: Cross-sectional Average Flow Velocity
u^+	: Nondimentional Velocity Parallel to the Wall
U_0	: Free Stream Velocity
U_f	: Friction Velocity
$\bar{u}$	: Time-averaged Velocity
u_i	: Particle Velocity
u'_i	: Fluctuating Part Of Particle Velocity
$\bar{u}_i$	: Mean Particle Velocity
U_m	: Eulerian Mean Velocity

$\sqrt{\overline{v'^2}}$: Turbulent Fluctiation
v’ : Velocity Fluctiation at y Direction
V : Flow Characteristic Velocity
$\boldsymbol{v}$: Kinematic Viscosity
w’ : Velocity Fluctiation at z Direction
w : Fall Velocity
x : Distance
$\bar{\mathbf{x}}$: Time-averaged Distance
X : Nondimensional Distance
$\mathbf{y}^+$: Wall Coordinate
$\Delta\mathbf{y}^+$: Coordinate Shift

LIST OF TABLES

Page

LIST OF FIGURES

Page

LONGITUDINAL DISPERSION OF HEAVY PARTICLES IN A FREE SURFACE FLOW OVER ROUGH BED

SUMMARY

Turbulent flow has been observed by humans throughout history, and was studied by science since at least the time of Leonardo Da Vinci. Although it is yet to be fully explained, causes and effects of this natural phenomenon are covered to an extent that we are able to acquire viable and applicable data, via analytical or numerical models.

One significant result of turbulence is the dispersion of material along the flow, namely longitudinal dispersion. This is also being studied along with turbulence, as it has a very significant practical importance; being very closely related to environmental pollution.

This study intends to numerically solve the dispersion of heavy particles in free surface flows over rough beds, and acquire accurate results compared to those of the physical experiments. Previous models numerically solved the turbulent dispersion of heavy particles over smooth bed. Most importantly, this study will be investigating the effect of rough beds on the dispersion. The software product of this thesis will be using somewhat refined methods from the previous ones to determine the variants used to calculate the dispersion. Finally, longitudinal dispersion coefficients for particles with different settling velocities in a free surface flow with various bed roughness values are intended to be acquired.

The law of the wall by Theodore Von Karman (1930), and the Van Driest velocity profile and the turbulent diffusion and dispersion physics lie fundamentally in the background of this study.

Random walk method will be modelled numerically for this thesis to use one particle analysis to determine dispersion coefficients for different variations of particle settling velocities and bed roughness values. What we will need is the velocity profile across the cross-section of the flow, the wall-normal turbulence velocities and particle behavior at the upper and lower boundaries (bed and surface).

For the mean x velocity, Van Driest profile has to be corrected with a wake function to be valid across the whole section of the flow. Present model will also be using Cebeci and Chang (1978) coordinate shift to inspect roughness effect on dispersion, which has never been applied on a numerical model before.

For wall-normal turbulence, the model will be using Nezu and Nakagawa (1993) semi-theoretical curve based on experimental data, modified to cover the inner region of the flow by Kirca (2013)

For heavy particles, a characteristic parameter representing the effect of gravity, called the Rouse parameter will be used.

As the particles will be moving upwards and downwards randomly along the cross section of the flow for the random walk method, we will be using a scale to determine

the length of this movement, namely the penetration length scale, which is basically the vertical size of the turbulent eddy, which carries the particle vertically. The model will be using Sayre (1968) and Sumer (1973) approximation of this length scale, smoothened by Kirca (2013) for using continuous and a differentiable value across the depth, with a tangent-hyperbolic function.

Particles will encounter flow boundaries across the way. They will be considered to bounce back into the flow. For any energy loss that would occur in nature, the model will be using a tuning parameter. To model the bouncing effect, a piecewise function by Kirca (2013) will be used.

The model is tested for naturally buoyant particles over smooth bed, for various Ref values from 500 to 50000, for heavy particles such as β = 0.1, 0.2, 0.3, 0.4, 0.5, 0.6, 0.7, 0.8, 0.9, 1 and 1,5 over smooth wall ($k_s^+ < 5$) and for k_s^+ roughness values from 5 to 2000 and β = 0.1, 0.2, to 0.9 and 1.

The software model seems to provide results that agree with the previous studies both numerical and analytical.

As for the innovative part of this study, Cebeci-Chang coordinate shift was included in the model along with the Coleman and Alanso wake function correction to have a refined profile and be able to inspect the effect of bed roughness on the dispersion of the heavy particles. Results show that, for neutrally buoyant particles, as roughness increases, dispersion coefficient tends to slightly decrease, especially when the roughness elements penetrates deeper into the flow domain (i.e. for high ks/h values). As the settling velocity of the particles increase, however, the effect of roughness on the dispersion seems to fade.

SERBEST YÜZEY AKIMINDA PÜRÜZLÜ TABAN ÜZERİNDE AĞIR PARÇACIKLARIN BOYUNA DİSPERSİYONU

ÖZET

Türbülanslı akım, tarihten bu yana insanlar tarafından gözlenmiş, ve en azından Leonardo Da Vinci döneminden beri bilimsel olarak incelenmiştir. Tam manasıyla açıklanmış olmasa bile, nedenleri ve sonuçları üzerinde hatırı sayılır sonuçlar elde edilmiştir. Öyle ki; bugün analitik ve numerik çalışma ve modellemelerle tutarlı ve uygulanabilir veriler elde edebilmekteyiz.

Modern türbülans araştırmalarının, Osborne Reynolds (1983) tarafından yapılan deneysel çalışmalarla başladığı söylenebilir. Reynolds, akımın karakteristik özelliklerini ifade eden boyutsuz bir sayıya bağlı olarak, akım rejiminin laminer ve türbülanslı olarak değiştiğini gözlemlemiştir. Bu sayıya Reynolds Sayısı denir.

Bir sonraki kilometre taşı, Ludwig Prandtl (1904) tarafından, sınır tabaka teorisi ile konmuştur. Sınır tabaka akışın, akışkanın vizkoz kayma gerilmelerinden önemli ölçüde etkilendiği bölgedir. Akışkanlar mekaniğinin gelişimi açısından büyük önem taşıyan bu teori, o dönemde hidrodinamik çalışmalar için sınırlı ölçüde kullanılmıştır. Bunun sebebi gelişen uçak teknolojisi ve bu endüstrinin yüksek ölçüdeki ihtiyacıdır. Bu ihtiyaç, akışkanlar mekaniği çalışmalarını aerodinamik alana yoğunlaştırmıştır.

Daha sonra Taylor (1935), gelişen ölçüm tekniklerinin de yardımıyla, bir "ideal türbülans" modeli olan izotropik türbülans kabulünü ortaya atmıştır. Bundan yola çıkan Kolmogorov (1941) iyi bilinen "-5/3" kanununu ortaya atmıştır.

Türbülans, Kline (1967) tarafından bulunan türbülans patlama olgusuna kadar, rastgele ve kaotik bir doğal fenomen olarak görülüyordu. Ancak bu olgunun öngörülebilir periyotlarla meydana gelmesi bu görüşü sorgulamıştır.

Türbülanslı akışın önemli bir sonucu olan boyuna dispersiyon, çevre kirliliği ile olan yakın ilişkisi sebebiyle özel bir pratik önem arz etmekte olup, birçok çalışmaya konu olagelmiştir. En önemli ve öncü çalışmalardan birisi Elder (1959) tarafından yapılmıştır. Elder, parçacıkların düşey pozisyonlarının olasılık yoğunluğu ve kanal kesiti boyunca parabolik bir hız dağılımı kullanarak parçacıkların ortalama hızını ve dispersiyon katsayısını hesaplamıştır. Bu çalışmada da Elder'ın (1959) sonuçlarına yer verilecektir. Bunun yanında Sayre (1968), Sumer (1974) ve Bayazıt (1972) önemli numerik çalışmalar yapmışlardır. Ayrıca Deng ve Jung (2008) ve Riahi-Madvar ve diğ. (2008) daha yeni çalışmalar yapmışlardır. Ancak geçmişte yapılan çalışmalarda taban pürüzlülüğünün etkisine yer verilmemiştir.

Bu çalışma, pürüzlü tabanlı açık kanal akımlarında, ağır parçacıkların boyuna dispersiyonunu sayısal bir model ile belirlemeyi amaçlamaktadır. Daha önce sayısal bir modelde kullanılmamış olan taban pürüzlülüğünün etkisi de bu tezin konusu olan yazılımla incelenecektir. Model, türbülanslı akış parametrelerini ve parçacık

hareketlerini belirlemek üzere, daha önce verilmiş ve analitik çözümlerde kullanılmış olan metodları rafine edilmiş ve yer yer geliştirilmş bir şekilde kullanacaktır.

Bu çalışmanın arka planında temel olarak Von Karman cidar kanunu ve Van Driest hız profili ile birlikte türbülanslı difüzyon ve dispersiyon fiziği bulunmaktadır.

Farklı çökelme hızı, taban pürüzlülüğü ve akım koşullarında dispersiyon katsayısını hesaplamak için, bu sayısal modelde rastlantısal yürüyüş metodu ile tekil parçacık analizi yapılacaktır. Bunun için gerekli olan; iki boyutlu akım düşey kesiti boyunca ortalama hız profili, cidara dik türbülans hızları ve cidar ve serbest yüzeyde parçacıkların davranışının modellenmesidir.

Ortalama hız profili için; Von Karman cidar kuralında belirtilen akışmaz alt tabaka, geçiş tabakası ve logaritmik tabakayı tek bir ifadede kapsayan Van Driest hız profilinden yola çıkılmıştır, ancak Van Driest Profili'nin logaritmik tabakadan sonra, tüm akım kesiti için geçerli olabilmesi için bir iz (wake) fonksiyonu ile düzeltilmesi gerekmektedir. Ayrıca, modelde incelenecek olan taban pürüzlülüğü için, Nikuradse eşdeğer kum pürüzlülüğü ifadesinin bir fonksiyonu olan Cebeci ve Chang (1978) koordinat kayması da bu ifade içerisine alınmıştır.

Cidara dik türbülans hızları için Nezu ve Nakagawa (1993) yarı teorik eğrileri, sınır tabakası iç bölgesini kapsaması için geliştirilerek kullanılmıştır. Ağır parçacıklar için ise çökelme hızını ifade eden karakteristik bir parametre olan Rouse Parametresi kullanılmıştır. Parçacıkların cidara dik hızlarının bulunması için, türbülans hızı, ortalaması 0 ve standart sapması 1 olan bir gauss rastgele sayısıyla çarpılmış ve Rouse parametresinden çekilen çökelme hızı eklenmiştir.

Parçacıklar rastlantısal olarak akım kesitinde yukarı ya da aşağı hareket edeceklerdir. Parçacıkların dikey yönde hareket uzunluğu; türbülans çevrintilerinin genişliği ile aynı olacaktır. Bu uzunluğun belirlenmesi için de Sayre (1968) ve Sümer (1973) tarafından yaklaşık olarak verilmiş değerler, bir tanjant hiperbolik eğri ile kullanılmıştır. Bu hareket uzunluğu ve parçacıkların dikey hızından yararlanılarak, rastlantısal yürüyüş adımının süresi hesaplanmıştır. Her parçacık, her rastlantısal yürüyüş adımında, dikey hareketi boyunca geçtiği hız profili bölgesine uygun yatay hız kazanır. Bu ortalama yatay hız ile rastlantısal yürüyüş adımının süresi çarpıldığında parçacığın o adımda katettiği yatay mesafe bulunur. Önceden belirlenmiş bir süre sonunda, her parçacığın katettiği yatay mesafe farklıdır. Bu mesafelerin varyansından yola çıkarak dispersiyon katsayısına ulaşılır.

Düşey hareketi esnasında cidar ya da serbest yüzeyle temas eden parçacıklar, bu yüzeylerden sektiği düşünülerek modellenmiştir. Parçacığın herhangi bir enerji kaynına uğramadan akım sınırından sektiği varsayılmıştır. Bu durumda normalde meydana gelebilecek enerji kayıplarını kapsayabilmek için bir ayar parametresi kullanılmıştır. Ayar parametresi, parçacığın düşey hızının belirlendiği, rastgeleliğin uygulandığı ifadeye eklenmiştir. Parçacıkların, akımın laminer olduğu, dolayısı ile yukarı yönde bir hızın oluşmadığı viskoz alt tabakada kalması engellenmiştir.

Pratiklik açısından Matlab, erişilebilirlik açısından da PHP, modelin oluşturulmasında kullanılmıştır. Performans açısından Matlab'ın üstün olduğu gözlenmiştir. Model her noktayı tekil olarak ve sırayla incelediğinden, incelenen nokta sayısı modelin performansı ve sonuca ulaşma süresi ile ters orantılıdır. Ancak nokta sayısı arttıkça daha sağlıklı ve tutarlı sonuçlar elde edilebilir. Bu sebeple bir optimum nokta sayısı belirlenmiş ve model bu nokta sayısıyla çalıştırılmıştır. Çalışmada verilen, kullanılan ifadeler ve akım şemasından yararlanarak, başka programlama dillerinde de modeli oluşturmak elbette mümkündür. Ayrıca daha güçlü bilgisayarlarda daha çok noktayla ve daha hızlı olarak sonuç alınabilir.

Model, 500 ile 50000 arasında değişen Reynolds sayıları için, pürüzsüz cidar üzerinde, askıdaki parçacıklar ile test edilmiştir. Daha sonra pürüzsüz yüzey üzerinde ağır parçacıklar ve son olarak da çeşitli pürüzlülüklerde, çeşitli ağırlıktaki parçacıklar ile test edilmiştir.

Pürüzsüz cidar ve askıdaki parçacıklar ile test edildiğinde, modelin Elder (1959) ve Sümer (1974) ile benzer sonuçlar verdiği görülmüştür.

Aynı şekilde, pürüzsüz cidar üzerinde, çökelme hızına sahip parçacıklar için modelden alınan sonuçların Sümer (1974) analitik çözümü ve Sayre (1968) sayısal çözümüyle paralellik arz ettiği görülmüştür.

Model, dispersiyon katsayısı üzerinde, cidar pürüzlülüğünün etkisini inceleyebilecek şekilde kodlanmıştır. Bu yönde daha önce yapılmış bir çalışma bulunmadığından herhangi bir karşılaştırma yapılamamaktadır. Model sonuçlarına göre; pürüzlülüğün genel olarak dispersiyon katsayısına etkisinin çok az olduğu söylenebilir. Ancak aynı Reynolds sayısında cidar pürüzlülüğü arttıkça dispersiyon katsayısının düşme eğilimi gösterdiği görülmüştür. Parçalar çökelme hızı kazandıkça cidar pürüzlülüğünün etkisinin ortadan kalktığı gözlenmiştir. Bunun sebebinin, parçacıkların daha hızlı çökelmesi, ve tabanda taşınması olduğu düşünülmektedir.

1. INTRODUCTION

1.1 Studies on Turbulence

Turbulence is a natural phenomenon, which is yet to be fully explained by physics, though it has been thought over and observed by scientists and curious human beings throughout history. One of the first written document on turbulence known to us is Leonardo Da Vinci's drawing of -presumed to be- himself observing the turbulent vortices and noting "Observe the motion of the water surface, which resembles that of hair, that has two motions: one due to the weight of the shaft, the other to the shape of the curls; thus, water has eddying motions, one part of which is due to the principal current, the other to the random and reverse motion." (Figure 1.1) with amazing precision of a genius observer. This probably makes him the first researcher of the open channel turbulence. He is also the first to use the word "turbulence" (turbolenza in Italian).

Figure 1.1 : Leonardo Da Vinci observing turbulent flow in his own drawing.

A modern study of the turbulence, however, was delayed until Osborne Reynolds (1883) experimentally expressed that fluids can flow in laminar or turbulent regime due to a dimensionless number, characterizing the flow environment, now called the Reynolds Number;

$$Re = \frac{LV}{\upsilon} \tag{1.1}$$

where L is the characteristic scale and V is the velocity of the flow, while υ is the kinematic viscosity.

Prandtl (1904) He presented the Boundary-Layer Theory, the layer close to the boundary of the flow where the fluid is significantly affected by viscosity.

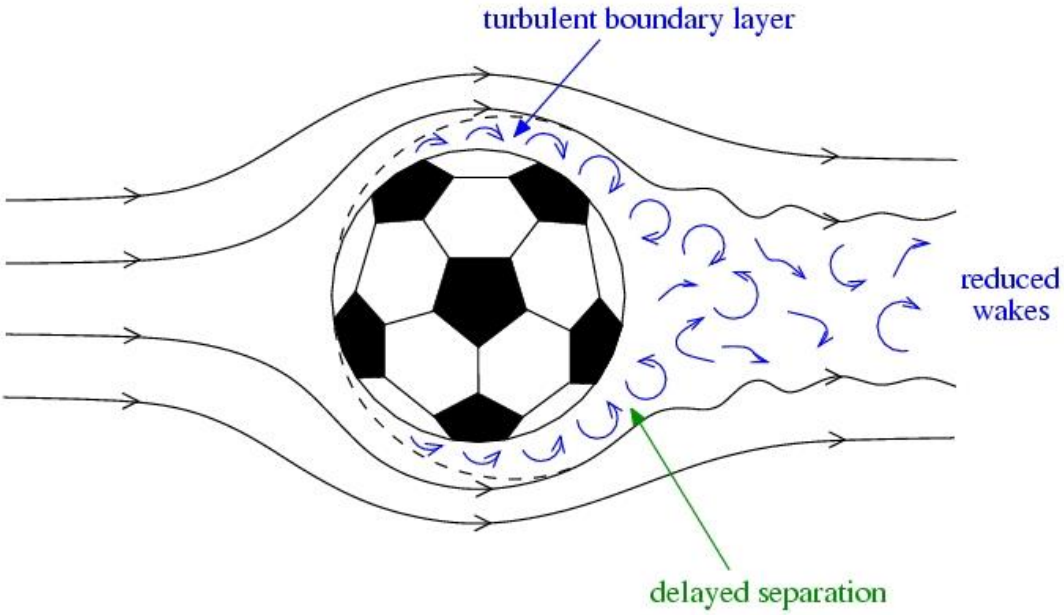

Figure 1.2 : Turbulent boundary layer (Yip, University of Hong Kong, The Science of Soccer Lecture Notes, 2012).

This theory was crucial to the airplane design, and the industry was very demanding at the time, so the concept was rarely applied in hydrodynamics. Another reason was that measuring of airflows was easier than the water flows. Boundary-layer theory contributed much to the development of aerodynamics. (Nezu and Nakagawa, 1993)

Development of turbulence research was strongly tied to the measurement techniques. In 1930's, hot-wire anemometry enabled researchers to measure airflow. The technique simply uses a platinum or tungsten wire heated to some temperature, and as the airflow cools the wire, the flow is measured by the changing electrical resistance of the metal, which is related to its temperature.

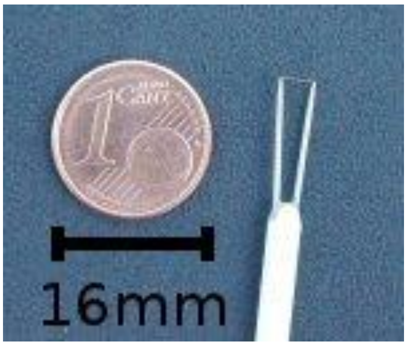

Figure 1.3 : Hot-wire sensor (wikipedia.com).

This simple device let Taylor, a great fluid mechanist; propose an “ideal turbulence” model, named isotropic turbulence in 1935. This had fundamental importance, as it led the way for the statistical theory of locally isotropic turbulence proposed by Kolmogorov (1941), which led to the well-known -5/3 power law for the spectrum of shear-flow turbulence. This theory could then be applied to real turbulent flows like those in boundary layers, pipe flows, jets and wakes, and even to the atmospheric turbulence and ocean turbulence. The theory can also be applied to open channel turbulence.

Until the discovery of the bursting phenomena in boundary layers by Kline (1967), and vortex-pairing phenomena in turbulent mixing layers by Brown & Roshko (1974) and Winant & Browand (1974), turbulence was considered quite random and chaotic. These important findings challenged the established theory of randomness and chaos, as these are discovered to occur periodically.

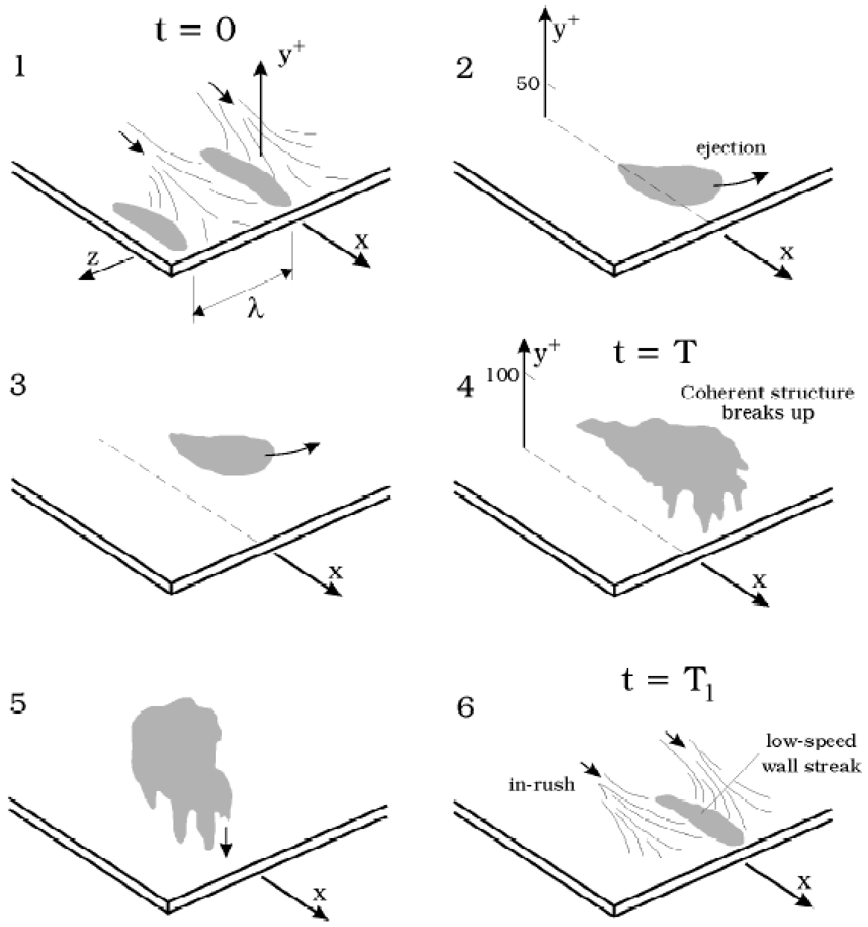

Figure 1.4 : Sequence of flow pictures over one bursting period (Sumer, 2007).

Mean bursting period is (Jackson, 1976);

$$\frac{T_1 U_o}{h} = 5 \qquad \textbf{(1.2)}$$

in which $\boldsymbol{U_o}$ is the free stream velocity.

In 1970's, the developing computer technology allowed significant progress in numerical fluid mechanics. Moin & Kim (1982) first simulated bursting motions near the wall using "Large Eddy Simulation" (LES) technique, however the results did not agree quantitatively with experimental data; hence Kim (1987) solved the Navier-Stokes equation numerically without any turbulence modelling. This is called the "Direct Numerical Simulation (DNS). Results of this study provide explanation for bursting motions both qualitatively and quantitatively (Nezu and Nakagawa, 1993). As new observation techniques and faster computers are available, more accurate and precise studies on this natural phenomenon are possible.

1.2 Studies on Turbulent Dispersion

Batchelor, Binnie and Phillips (1955) studied the mean velocity and the longitudinal dispersion of particles in a circular pipe and showed that the time-averaged axial component of velocity of a fluid particle is equal to the discharge velocity. Binnie and Phillips (1958) extended this work to cover slightly heavy and buoyant particles. Barnard & Binnie (1963) extended this study one-step further to include heavy particles.

Elder (1959) applied the analysis developed by Taylor (1954) to describe the longitudinal dispersion of discrete particles, both of zero and of finite buoyancy. Using the expression for the probability density of the particle position in the vertical and assuming a parabolic velocity distribution in the channel, Elder (1959) calculated the mean velocity of heavy particles and then predicted the dispersion coefficient. In predicting the dispersion coefficient, an expression derived from the equation of conservation of mass was used, which, in that case, did not contain a term characterizing the settling of particles due to gravity. Because an artificial velocity distribution was used in the calculation, and the main equation in the derivation of the expression for the dispersion coefficient should have had a fall velocity term, Elder's (1959) estimate differs from Sayre's (1968) numerical calculation.

Batchelor (1965), reviewed on the motion of small particles in turbulent flow, discussed the systematic effects of inertia difference or more important, the action of gravity on the motion of a heavy particle. In particular, he examined the equation representing the balance between transport due to gravity and turbulent transport near the bottom of an open-channel flow. From this, there can be obtained a criterion for whether the particles stay in suspension or not.

Sayre (1968, 1969) formulated the dispersion process of sediment particles in an open-channel flow in the Eulerian sense, permitting the exchange of particles by introducing a so-called bed absorbency coefficient and an entrainment-rate coefficient. Using the Aris moment transformations, he obtained zeroth, first, second and third moments of the concentration numerically with the aid of a digital computer. Sumer (1971) examined the specific case in which the ratio of the fall velocity of particles to the shear velocity is small compared with unity, which probably implies that the particles are all transported in suspension and the mean particle velocity is approximately equal to that of the flow. Applying the method used by Taylor (1954), he obtained an expression for the longitudinal dispersion Coefficient (Sumer, 1974).

When measurements and real data of mixing processes in river are available, the longitudinal dispersion coefficient is determined simply, but in rivers that the mixing and dispersing data is not available and these phenomena are not known, should use alternative methods for estimation of dispersion coefficient values (Kashefipur and Falconer, 2002). In these cases, because of the complexity of mixing phenomena in natural rivers, the best estimations of dispersion coefficients are not possible and usually these values are determined by several simple regressive equations (Deng et al., 2001). There are several empirical equations for estimation of longitudinal dispersion coefficient (Seo & Cheong, 1998). Examples are given in Table 1.1, where D_1 is the longitudinal dispersion coefficient, B is the longitudinal scale, H is the depth average of flow in cross section, U_f is the friction velocity and $\boldsymbol{\varepsilon_t}$ is the cross sectional average of transverse mixing coefficient.

Table 1.1 : Empirical equations for estimation of longitudinal dispersion coefficient. (Riahi-Madvar et al., 2008)

Equation	Author
$D_1 = 5.93HU_f$	Elder, 1959
$D_1 = 0.58\left(\frac{H}{U_f}\right)UB$	McQuivey and Keefer, 1974
$D_1 = 0.011\left(\frac{U^2B^2}{HU_f}\right)$	Fisher, 1967
$D_1 = 0.55\left(\frac{BU_f}{H^2}\right)$	Li et al., 1998
$D_1 = 0.18\left(\frac{U}{U_f}\right)^{0.5}\left(\frac{B}{H}\right)^{2}HU_f$	Liu, 1977
$D_1 = 2.0\left(\frac{B}{H}\right)^{1.5}HU_f$	Iwasa and Aya, 1991
$D_1 = 5.92\left(\frac{U}{U_f}\right)^{1.43}\left(\frac{B}{H}\right)^{0.62}HU_f$	Seo and Cheong, 1998
$D_1 = 0.6\left(\frac{B}{H}\right)^{2}HU_f$	Koussis and Rodriguez-Mirasol, 1988
$D_1 = 0.2\left(\frac{U}{U_f}\right)^{1.2}\left(\frac{B}{H}\right)^{1.3}HU_f$	Li et al., 1998
$D_1 = \frac{0.15}{8\varepsilon_t}\left(\frac{U}{U_f}\right)^{2}\left(\frac{B}{H}\right)^{1.67}HU_f$ $\varepsilon_t = 0.145 + \frac{1}{3520}\frac{U}{U_f}\left(\frac{B}{H}\right)^{1.38}$	Deng et al., 2001
$D_1 = 10.612\left(\frac{U}{U_f}\right)HU$	Kashefipur and Falconer, 2002
$D_1 = 7.428 + 1.775\left(\frac{B}{H}\right)^{0.62}\left(\frac{U}{U_f}\right)^{1.572}HU$	Kashefipur and Falconer, 2002

Beer and Young (1983) proposed that the effects of dispersion in natural streams can be modelled by an aggregated dead zone model, in which each reach of the river is treated as being composed of a length in which the dispersant solute undergoes pure translational (plug) flow with a certain concentration and enters a “mixing tank” and emerges with a different concentration.

The following form of the transient storage (TS) model (Nordin and Troutman, 1980; Bencala and Walters, 1983; Schmid, 1995; Harvey et al., 1996, Runkel, 1998) often describes the longitudinal transport process of pollutants in natural rivers without lateral inflow or outflow:

$$\frac{\partial \overline{c}}{\partial t} + U\frac{\partial \overline{c}}{\partial x} = Ks\left(D_x\frac{\partial^2 \overline{c}}{\partial x^2}\right) + \frac{A_s}{A}\frac{1}{T_C}(C_S - C) \qquad \textbf{(1.3)}$$

$$\frac{\partial C_S}{\partial t} = \frac{1}{T_C}(C_S - C) \qquad \textbf{(1.4)}$$

where C is the solute concentration in main channel, C_S is the solute concentration in storage zones, T_C is the main residence time of solute in storage zones, K_S is the longitudinal Fickian dispersion coefficient excluding the transient storage effect, t is time and t = 0 corresponds to the instant when a pollutant or tracer is released; x is distance and x = 0 corresponds to the location where a pollutant or tracer is released; U is cross-sectionally averaged flow velocity; A is cross-sectional flow area of main channel; A_S is cross sectional area of transient storage zone, $A_S/A = R$ is the ratio of transient storage zone volume per unit length to main stream volume per unit length. Eq. (1.3) holds after the initial mixing period or for the far field where the longitudinal shear flow dispersion becomes a dominant mechanism of solute mixing. In addition to the shear flow dispersion, transient storage in in-channel dead zones and/or out-of-channel hyporheic zone is also an important mechanism responsible for the longitudinal dispersion and transport of solute in natural streams and rivers. The TS model takes into account both the shear flow dispersion and transient storage effect in in-channel dead-zones and/or out-of-channel hyporheic zone (Zhi-Qiang Deng and Hoon-Shin Jung, Scaling dispersion model for pollutant transport in rivers, 2008).

Deng and Jung (2008), presented a transient storage model for solute transport in natural rivers without using any user-specified residence time distribution functions. The model was characterized by a scale-dependent residence time and is called scaling dispersion model. Riahi-Madvar et. al. (2008) also develeoped a tool to predict longitudinal dispersion using adaptive neuro-fuzzy inference system (ANFIS).

One significant study is done by Bayazıt (1972), in which he used a random walk model to determine settling lengths of particles realeased from the free surface of an free surface flow with fully developed turbulence. His study considered micro scales of turbulence, and the flow bed was defined as absorbing barrier, while the surface was defined as the reflecting barrier, therefore no reflection from the flow bed was taken into account. His study is particularly useful in the design of settling basins.

Note that none of these previous models inspected the roughness effect on dispersion, as done by the model presented in this study.

1.3 Importance of Turbulent Dispersion

Almost all of the flows we encounter in our everyday lives or for engineering problems are turbulent. And most frequently, they are carrying particle masses that we would very much like to know where they're going. The most obvious example is a pollutant mass inside a fluid current; for example a river, an ocean or the atmosphere. And particles caused by marine dredging operations, settling basins, transport of suspended matter to coastal regions by streams etc. can be given as example to the dispersion of heavy particles. As it is almost impossible to keep these pollutants away from the fluids; efforts for keeping the pollution contained inside tolerable boundaries may begin with the knowledge of how and where the material is going.

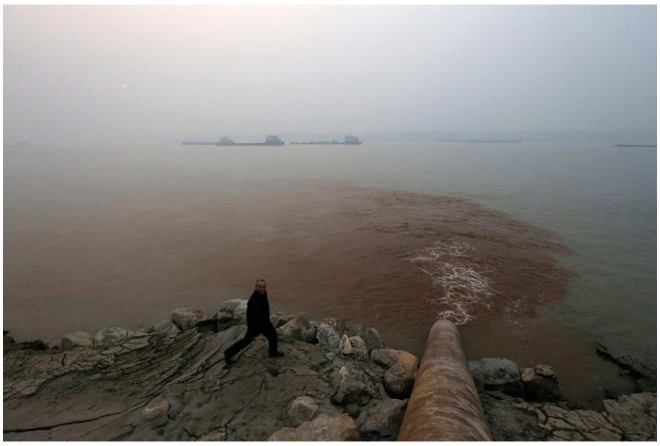

Figure 1.5 : Pollutant Dispersion Inside Water (China).

1.4 Purpose of This Thesis

This study intends to numerically solve the dispersion of heavy particles in free surface flows over rough beds, and acquire accurate results compared to those of the physical experiments. Numerically solving this problem is important because, marine dredging operations, coastal sediment transported by rivers and streams, modelling for structure and facility planning, waste management etc. may require having results for a lot of variation of situations, and computer aid in acquiring those is essential for time saving and accuracy. Therefore, the numerical models used for this purpose should be fine-tuned and improved continuously.

1.5 Scope of The Study

Previous models numerically solved the turbulent dispersion of heavy particles over smooth bed. Most importantly, this study will be investigating the effect of rough beds on the dispersion. The software product of this thesis will be using somewhat refined methods from the previous ones to determine the variants used to calculate the dispersion. Finally, longitudinal dispersion coefficients for particles with different settling velocities in a free surface flow with various bed roughnesses are intended to be acquired. The combined effect of fall velocity, bed roughness as well as Reynolds number could be evaluated with the proposed numerical modelling study.

2. BACKGROUND

2.1 Velocity Fluctuations

The mean value of the velocity of the flowing particle is, like every other hydrodynamic quantity, given by;

$$\bar{u_i} = \frac{1}{T}\int_{t_0}^{t_0+T} u_i \, dt \qquad \textbf{(2.1)}$$

where t_0 is the arbitrary time, and T is the timespan which the mean velocity is measured. This is called time averaging (Sumer, Rev.2007).

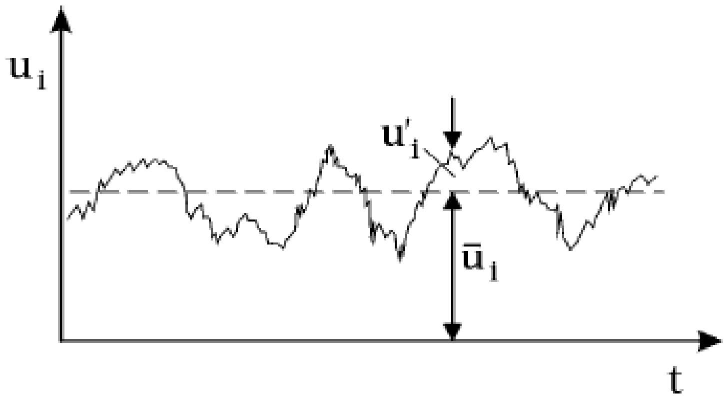

Figure 2.1 : u_i time series (Sumer, 2007).

As can be seen in Figure 2.1, any instantaneous value of the velocity can be calculated;

$$u_i = \bar{u_i} + u_i^{'} \qquad \textbf{(2.2)}$$

$\boldsymbol{u_i'}$ is called the fluctuation of $\boldsymbol{u_i}$, and $\boldsymbol{\overline{u_i}}$ is the mean value of $\boldsymbol{u_i}$. This is called the Reynolds decomposition. The Reynolds decomposition can be applied to any hydrodynamic quantity (B. M. Sumer, 2007).

The velocity of any single particle is essentially that of the stream line on which it is located, a function of cross-sectional position. Because of the molecular diffusion and the turbulence velocities perpendicular to the flow direction, each particle moves at random back and forth across the cross-section (Fischer, 1979). Given the velocity profile across the section, the velocity fluctuation along the flow direction is a function of cross sectional position.

Since a 2D flow is assumed in this study, the mean velocity values of y and w are considered 0.

2.2 Mean Flow and Turbulence in a 2D Free Surface Flow

2.2.1 Law of the wall

The Law of The Wall, published by Theodore Von Karman (1930), states that; the mean velocity of turbulent flow at a certain point can be calculated using the logarithm of the vertical distance of that point to the wall. However, inside the viscous sublayer, which can be defined as the layer so close to the boundary of fluid region so that the flow is laminar, the mean velocity of the turbulent flow is linear to the vertical distance.

The wall coordinate;

$$y^{+} = \frac{y\, U_f}{\nu} \qquad \textbf{(2.3)}$$

is the dimensionless vertical distance from the wall, where *y* is the distance from the wall, U_f is the friction velocity and *v* is the kinematic viscosity of the fluid.

Viscous sublayer is where y^{+}< 5. In this region, the mean velocity is linear to the distance to the wall;

$$u^{+} = \frac{u}{U_f} = y^{+} \qquad \textbf{(2.4)}$$

where u is the velocity parallel to the wall.

For y^{+}> 60, this region is called the "logarithmic layer" where the average velocity of the flow is;

$$u^{+} = 2.5 \ln y^{+} + 5.1 \qquad \textbf{(2.5)}$$

Thus, the velocity profile, according to the law of the wall is as shown in Figure 2.2.

The region where $\boldsymbol{y^{+}}$ is between 5 and 60 is called the buffer layer; where neither of the velocity profiles apply.

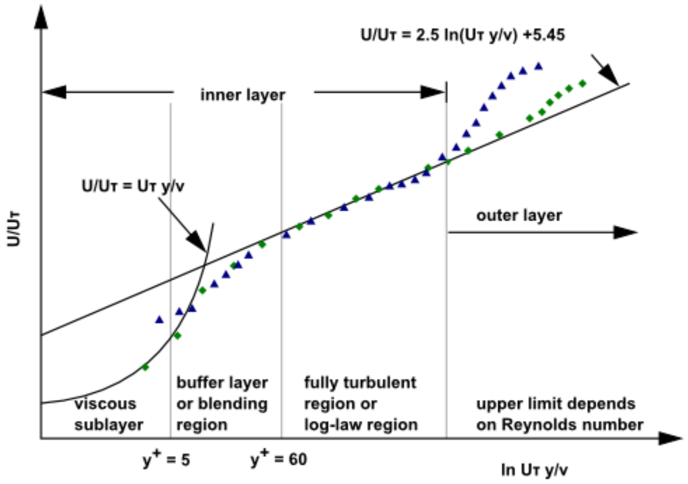

Figure 2.2 : Velocity distribution according to the law of the wall.

2.2.2 Van Driest profile

Van Driest (1956) introduced a velocity which is called the Van Driest Profile;

$$\bar{u} = 2U_f \int_0^{y^+} \frac{dy^+}{1 + \left\{1 + 4\kappa^2 y + 2\left[1 - \exp\left(-\frac{y^+}{A_d}\right)\right]^2\right\}^{1/2}} \qquad \textbf{(2.6)}$$

Where $\boldsymbol{A_d}$ is the damping coefficient and taken as ≈25. The resulting velocity profile is shown in figure 2.3.

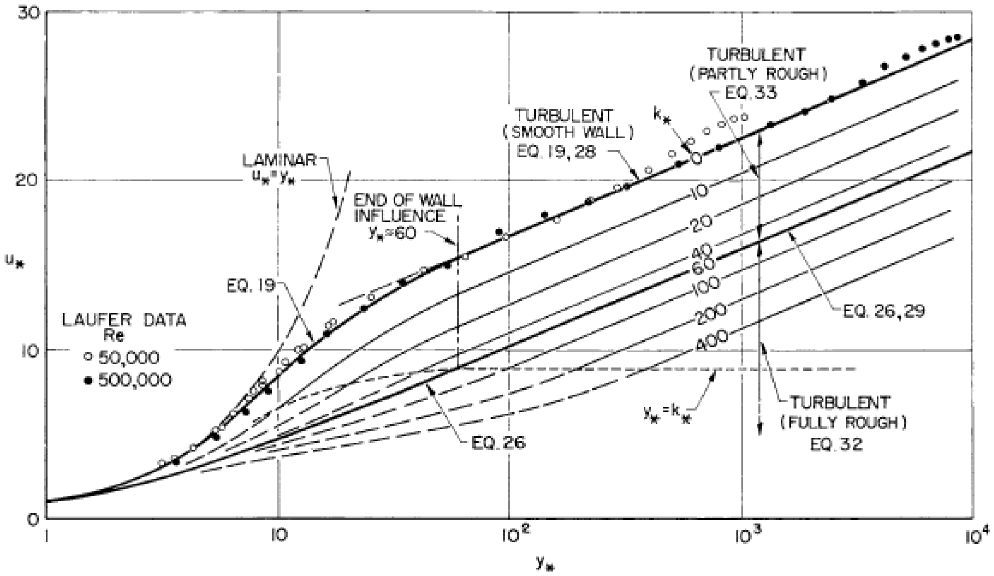

Figure 2.3 : Van Driest velocity profile for different rougness values, (Van Driest, 1956)

2.3 Turbulent Diffusion and Dispersion

2.3.1 Turbulent diffusion

If a certain amount of particles are to be placed into one point in a turbulent flow; because of turbulence, particles would start to move away from each other and all particles would move towards a different way, causing the particles to form a growing cloud. This is called turbulent diffusion, an it is defined as;

$$\frac{\partial \bar{c}}{\partial t} + \bar{u}\frac{\partial \bar{c}}{\partial x} + \bar{v}\frac{\partial \bar{c}}{\partial y} + \bar{w}\frac{\partial \bar{c}}{\partial z} = \frac{\partial}{\partial x}\left(D_{1_x}\frac{\partial \bar{c}}{\partial x}\right) + \frac{\partial}{\partial y}\left(D_{1_y}\frac{\partial \bar{c}}{\partial y}\right) + \frac{\partial}{\partial z}\left(D_{1_z}\frac{\partial \bar{c}}{\partial z}\right) \quad \textbf{(2.7)}$$

in which c is the concentration and D_1 is the turbulent diffusion coefficient in respective axes.

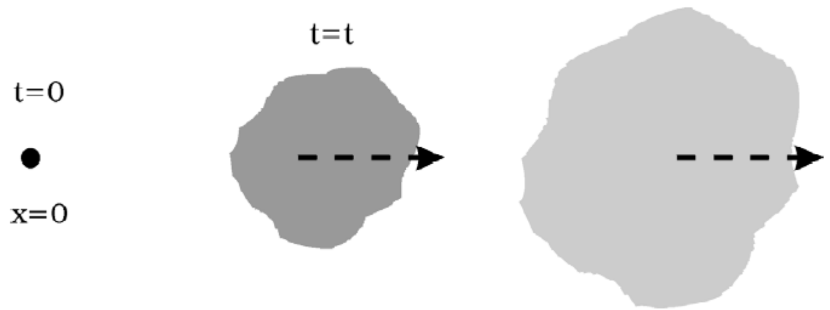

Figure 2.4 : Diffusion (Sumer, 2007).

2.3.2 Turbulent dispersion

Particles, initially present at a starting $x = 0$ point in a turbulent flow, will be moved along the flow direction with the flow velocity. And because of the wall-normal turbulence velocities, they will make random movements vertically across the cross section of the flow. As the mean velocity differs across the cross section, every particle will move with the speed of the layer it is in at the time. Hence, after a certain time, each particle will have travelled different ranges along the flow direction. This will cause the particle cloud to disperse; and this is called turbulent dispersion; defined as;

$$\frac{\partial < c >}{\partial t} + U_m\frac{\partial < c >}{\partial x} = D\frac{\partial^2 < c >}{\partial x^2} \quad \textbf{(2.8)}$$

in which $\boldsymbol{D}$ is the dispersion coefficient, $\boldsymbol{U_m}$ is the Eulerian mean velocity and $< \boldsymbol{c} >$ is the cross-sectional average concentration:

$$< c > = \frac{1}{h}\int_0^h \bar{c}dy \quad \textbf{(2.9)}$$

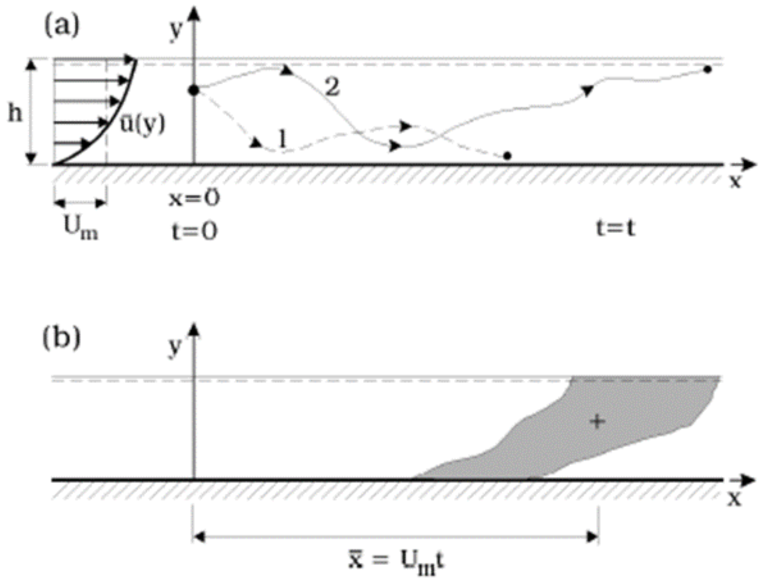

Figure 2.5 : Longitudinal Dispersion (Sumer, 2007).

3. METHOD

3.1 The Random Walk Method

Suppose that the motion of a tracer molecule or particle consists of a series of random steps. Although in reality the motion is in three dimensions, nothing important is lost if for the moment we assume that the motion is one dimensional. Assume further that each step is of equal length Δx and takes an interval of time Δt, but that whether the step is forward or backward is entirely random with equal probability. We ask how far the particle is likely to get; on the average, the answer is nowhere, but after a number of steps, sometimes the particle will have moved forward and sometimes backward (Fischer, 1979). Assume equally distributed particles are placed along the cross section at the starting point. Random walk method deals with every single particle separately and traces it for given timespan with randomized steps back and forth the cross section. Particle speed changes according to the velocity profile, so every particle has its own travel distance X. What we are trying to acquire is the variance of X, which will lead us to the dispersion coefficient.

$$D_1 = \frac{1}{2}\frac{d\overline{(X-\overline{X})^2}}{dt} \tag{3.1}$$

where D_1 is the dispersion coefficient and X is the final particle travel distance from the starting point.

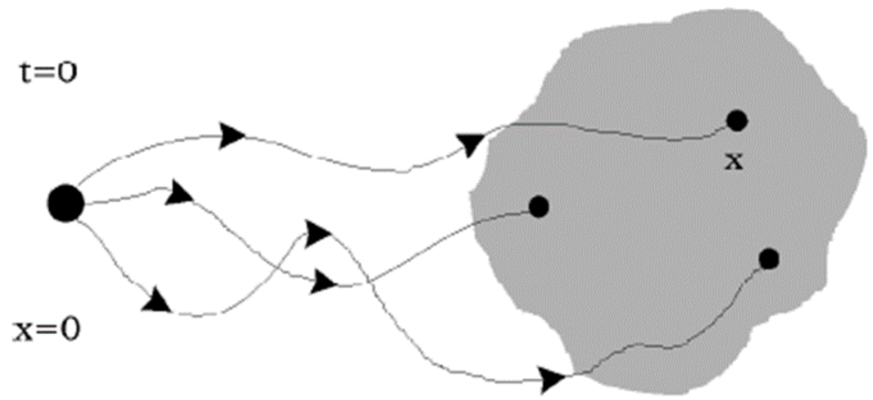

Figure 3.1 : Random Paths of Particles (B. M. Sumer, 2007).

3.2 Present Model

The random walk method will be implemented numerically to determine the dispersion coefficient for various particle densities and bed roughnesses; and intending to finally achieve correct results for heavy particles over rough bed in a free surface flow. For starting condition; N number of particles will be distributed evenly between the free surface and lower flow boundary at t=0 time and x=0 position. Then the particles will be released into the flow one by one and traced until a t=T time. The average and variance of the final positions of the particles will be used to analyse dispersion. What we will be needing is the velocity profile across the cross-section of the flow, the wall-normal turbulence velocities and particle behaviour at the upper and lower boundaries (i.e. bed and surface).

3.2.1 Mean flow

For mean velocity profile; present model will be using the Van Driest profile (see 2nd part) modified with respect to Cebeci and Chang (1978) coordinate shift (Fig. 3.2) which is defined as;

$$\Delta y^{+} = 0.9\left[\sqrt{{k_s}^{+}} - {k_s}^{+}\exp\left(-\frac{{k_s}^{+}}{6}\right)\right] \;; \qquad 5 < {k_s}^{+} < 2000 \qquad \textbf{(3.2)}$$

in which $\boldsymbol{k_s}^{+}$ is the roughness Reynolds Number;

$${k_s}^{+} = \frac{k_s U_f}{\nu} \qquad \textbf{(3.3)}$$

where $\boldsymbol{k_s}$ is the Nikuradse's equivalent sand roughness. In the present model, this function is extended to cover the entire section by means of Coles' Wake Function (Coleman and Alanso, 1983) which is;

$$\left(\frac{\Pi}{\kappa}\right)\omega\left(\frac{y^{+}}{h^{+}}\right) = \left(\frac{\Pi}{\kappa}\right)2sin^{2}\left(\frac{\pi}{2}\frac{y^{+}}{h^{+}}\right) \qquad \textbf{(3.4)}$$

where Π is a wake strength coefficient, $\boldsymbol{h}$ is the flow depth/pipe radius or the boundary layer thickness (B. M. Sumer, Lect. Notes on Turbulence, Rev.2007), $\boldsymbol{y^{+}}$ is the dimensionless depth expression which is;

$$y^{+} = \frac{y\,U_f}{\nu} \tag{3.5}$$

ν is the kinematic viscosity and $\boldsymbol{U_f}$ is the friction velocity, defined by;

$$U_f = \sqrt{\frac{\tau_0}{\rho}} \tag{3.6}$$

where τ_0 is the bed shear stress. To apply this function to the Van Driest velocity profile with coordinate shift, it has to be corrected to produce a zero value of the derivative $\boldsymbol{d\bar{u}\,/\,dy}$ at pipe-centers and boundary layer flows. The final form of the velocity expression (including the corrected wake function) will be as follows (Coleman and Alanso, 1983);

$$\frac{\bar{u}}{U_f} = \int_0^{y^+} \frac{2dy^+}{1 + \left\{1 + 4\kappa^2 (y^+ + \Delta y^+)^2 \left[1 + exp\left(-\frac{(y^+ + \Delta y^+)}{A_d}\right)\right]^2\right\}^{\frac{1}{2}}} + \left(\frac{y^+}{h^+}\right)^2 \left(1 - \frac{y^+}{h^+}\right) + \left(\frac{2\Pi}{\kappa}\right)\left(\frac{y^+}{h^+}\right)^2 \left[3 - 2\frac{y^+}{h^+}\right] \tag{3.7}$$

in which A_d is the damping coefficient and taken as ≈25. Regarding the Π values, this parameter basically depends on two factors: (1) the driving pressure gradient, and (2) the degree of turbulence in the outer region. A convergent flow (favourable pressure gradient) tends to produce low values of Π, while a divergent flow (adverse pressure gradient) produces high values of Π. Likewise, if the turbulence in the outer region is intense, Π will have low values, while, the turbulence in the outer region is weak, Π will have large values (Coleman and Alanso, 1983). Π will range between 0 and 0,55. Present model will be using an empirical expression;

$$\Pi = \max\left(0,\;\; 0.19 \tanh\left(\frac{(Re_f - 440)}{500}\right)\right) \tag{3.8}$$

Eq. (3.8) has been approximated from the empirical curve suggested by Nezu and Nakagawa (1993). Here $\boldsymbol{Re_f}$ is the friction Reynolds number;

$$Re_f = \frac{h\,U_f}{\nu} \tag{3.9}$$

where h is the thickness of the boundary layer (i.e. depth of the channel). This expression gives a Π value of zero at $\boldsymbol{Re_f} < \mathbf{440}$ and 0.19 at $\boldsymbol{Re_f} > \mathbf{2000}$; an average value obtained by Coleman (1981) for free surface flows.

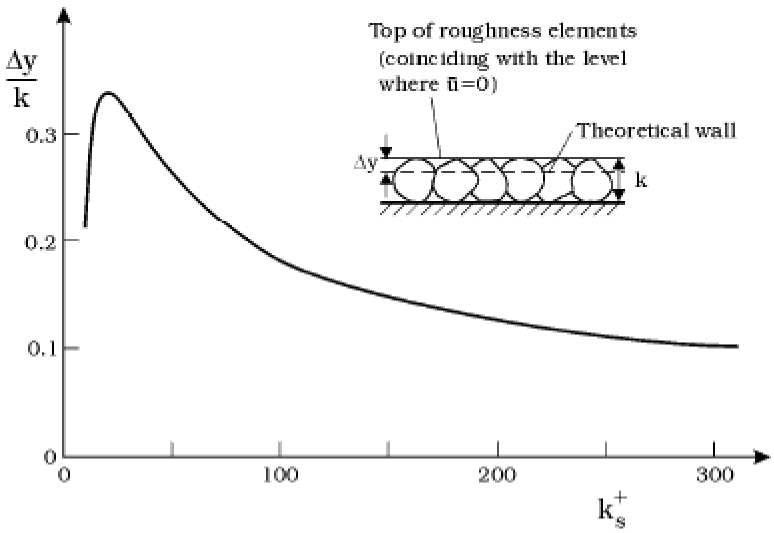

Figure 3.2 : Coordinate shift Δy from Rotta (1962) and Cebeci and Chang (1978), (Sumer, 2007).

3.2.2 Wall normal turbulence fluctuations

All three components of turbulence intensities u', v' and w' were first measured by Nakagawa (1975) for free surface flows using dual-sensor hot-film anemometers. Universal expressions for turbulence velocities, normalized with the friction velocity, were later investigated for various values of the Reynolds and Froude numbers in smooth free surface flows (Nezu and Nakagawa, 1993).

The effect of wall roughness on turbulence intensities was measured using a hydrogen-bubble technique by Grass (1971), and using hot-film anemometers by Nezu (1977) (Nezu and Nakagawa, 1993). The results can be seen in Figure 3.3.

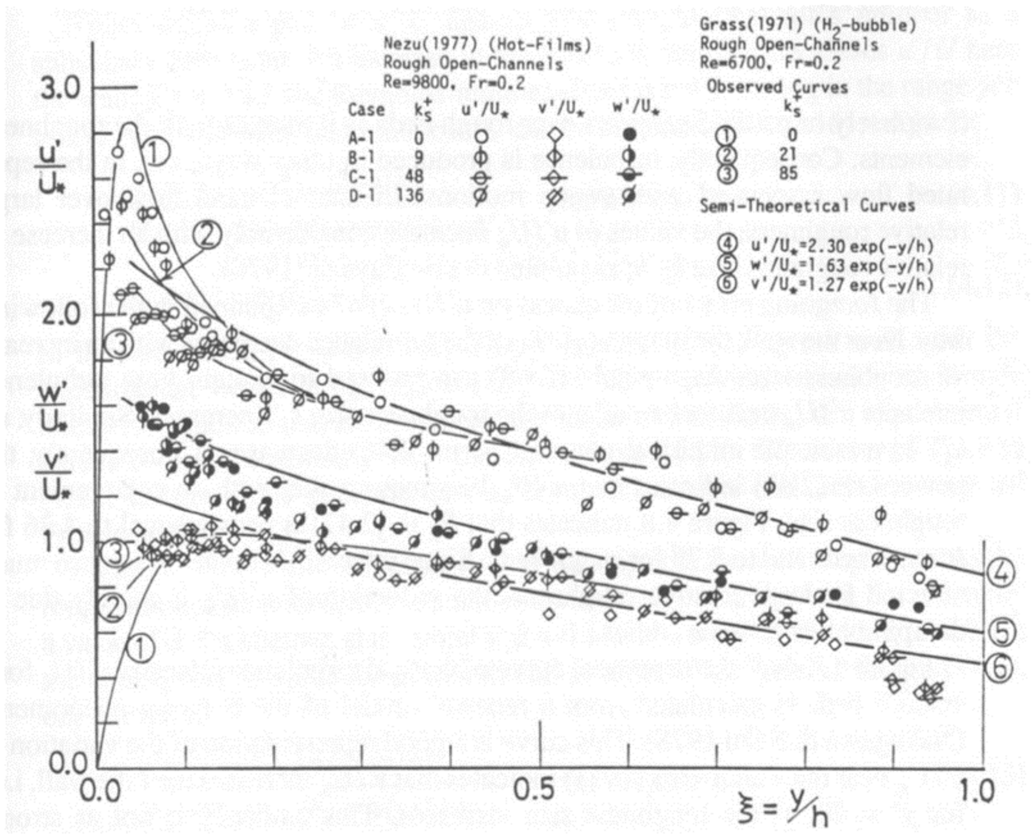

Figure 3.3 : Variation of turbulence intensities over smooth and rough beds as a function of (y/h) and roughness $\boldsymbol{k_s^+}$ (Nezu and Nakagawa, 1993).

As seen, wall-normal turbulence intensity is expressed with the semi-theoretical curve;

$$\frac{\sqrt{\overline{v'^2}}}{U_f} = 1.27\, exp\left(-\frac{y}{h}\right) \tag{3.10}$$

A version of the Eq. 3.10, modified by Kirca (2013a) will be used to cover the inner region turbulence intensity and give a zero value at y/h = 0. Which is as follows;

$$\frac{\sqrt{\overline{v'^2}}}{U_f} = 1.27\, exp\left[-\left(\frac{y}{h} + \frac{\Delta y^+}{Re_f}\right)\right]\left[1 - exp\left(\frac{-(y^+ + \Delta y^+)}{16}\right)\right] \tag{3.11}$$

The second part of Eq. 3.11 and $\frac{\boldsymbol{\Delta y^+}}{\boldsymbol{Re_f}}$ are added to cover the inner (near-wall) region of the flow since it is known that the near-wall turbulence is dependent on Reynolds number (for more details see chapter 2 in Sumer, 2007). The resulting curve can be seen at figure 3.4.

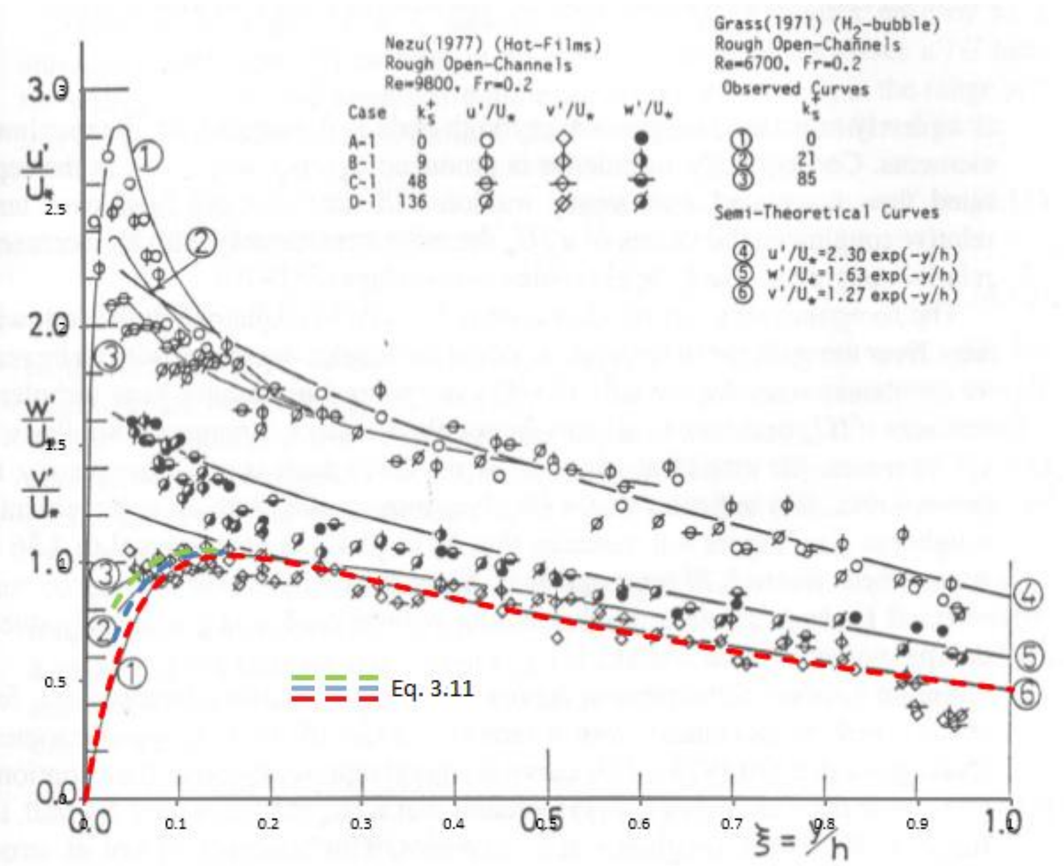

Figure 3.4 : Modified $\sqrt{\overline{v'^2}}$ curve (Kırca and Sumer, 2013).

For heavy particles, a characteristic parameter representing the effect of gravity, called the Rouse parameter (non-dimensional fall velocity) will be used;

$$\beta = \frac{w}{\kappa U_f} \tag{3.12}$$

where w is the fall velocity (Sumer, 1974). The final wall-normal velocity is determined by;

$$V = \left(a \frac{\sqrt{\overline{v'^2}}}{U_f} - w \right) b \tag{3.13}$$

where a is a Gaussian random number whose mean is 0 and standard deviation is 1, whereas b is a constant tuning parameter used to cover any energy losses, inertial differences etc.

3.2.3 Penetration length scale

The vertical travel distance of the particles, caused by turbulent eddies and randomized upwards or downwards in the Random Walk Method, is called the penetration length scale. The particle will move vertically along the cross section of the flow, assuming the velocity values of each layer it passes. Hence, the average velocity of the particle will be;

$$\bar{u}_{avg} = \frac{\int_{y_1}^{y_2} \bar{u}(y)dy}{|y_2 - y_1|} \qquad \textbf{(3.14)}$$

where $\boldsymbol{y_1}$ is the initial position of the particle, and $\boldsymbol{y_2}$ is the final position. And the time it will take to complete that particular random walk step will be;

$$\Delta t = \frac{l_p}{\sqrt{\overline{v'^2}}} \qquad \textbf{(3.15)}$$

where $\boldsymbol{l_p}$ is the penetration length scale and $\sqrt{\overline{\boldsymbol{v'^2}}}$ is the turbulence velocity. $\boldsymbol{l_p}$ is a turbulence length scale which can be defined as (Sumer, 1973);

$$\frac{l_p}{h} = \int_0^h \frac{\overline{u'(\lambda)u'(y)}}{\sqrt{\overline{u'^2}(\lambda)}\sqrt{\overline{u'^2}(y)}} d\lambda \qquad \textbf{(3.16)}$$

Sayre (1968) and Sumer (1973) approximated $\boldsymbol{l_p}$ as the following equation (3.17), stemming from the earlier experimental findings of Laufer. This is because, the penetration length is expected to be around the lagrangian macro scale, which is approx. 0.21 times the flow depth (Sayre, 1968), and as eddies get close to the boundaries, their scales will decrease accordingly.

$$\frac{l_p}{h} = \begin{cases} 0.21 \quad , & \frac{y}{h} > 0.21 \\ \frac{y}{h} \quad , & \frac{y}{h} \leq 0.21 \end{cases} \qquad \textbf{(3.17)}$$

For the sake of using a continuous and a differentiable value across the depth $\boldsymbol{l_p}$ is expressed as a tangent-hyperbolic function (Kirca, 2013), which is;

$$l_p = 0.21\left(\tanh\left(\left(\frac{y/h}{0.25}\right)^3\right)\right)^{1/3} \qquad \textbf{(3.18)}$$

This model will be used to achieve a round curve at 0.21 asymptote, resulting the profile in Figure 3.5.

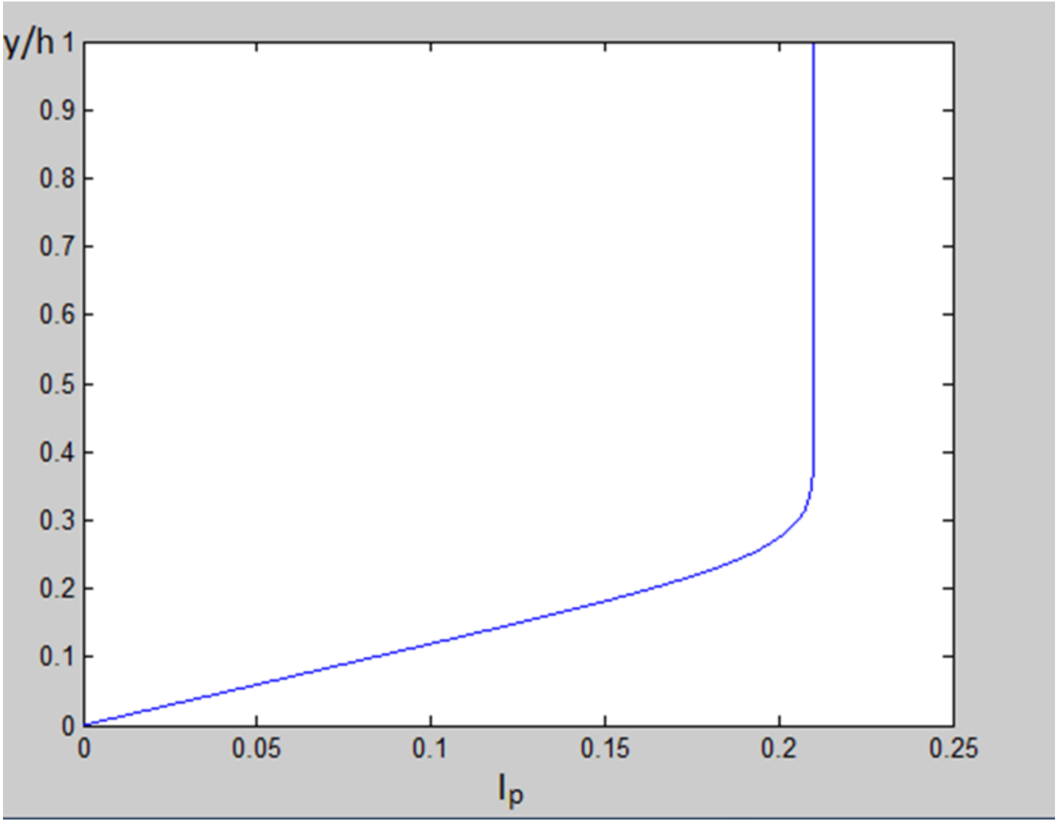

Figure 3.5 : Penetration length scale along the cross section of the flow.

Therefore, horizontal travel distance of the particle will be;

$$\Delta x = \bar{u}_{avg} \cdot \Delta t \tag{3.19}$$

The trace of a single particle can be seen in Figure 3.6.

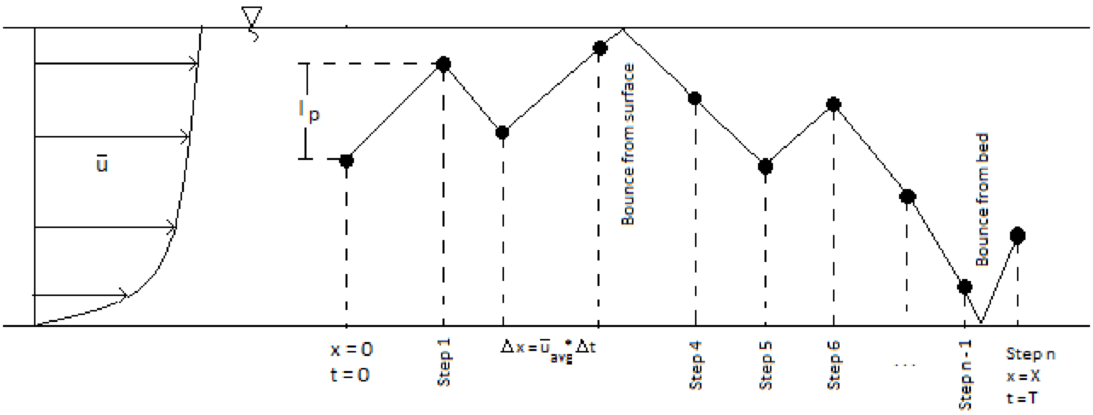

Figure 3.6 Particle trace.

3.2.4 Wall and free surface conditions

As the particles are traced in Random Walk Model, they will be moving randomly upwards and downwards along the cross-section of the flow (see 3.1). Therefore, they will sometimes intersect with flow boundaries. These are; flow bed (wall) and free surface for open channel and free surface flows, and pipe walls for pipe flows. As this study will be dealing with free surface flow, boundaries will be the prior ones.

When the particle intersects with flow boundaries, it is considered to bounce back. For the surface, this boundary is the upper layer that converges with the surface. And for the bed, the bouncing level is determined according to the coordinate shift (see 3.2.1). But in any case the particles are not let inside the viscous-sub layer.

To determine the new vertical position of the particle after the bouncing takes place following piecewise function will be used (Kirca, 2013);

$$y_2 = \begin{cases} y + \Delta y, & \delta_b < y + \Delta y < h \\ 2h - y + \Delta y, & y + \Delta y \geq h \\ max\{\delta_b, [2\,\delta_b - (y + \Delta y) - 2\,w_s\,\Delta t]\}, & y + \Delta y \leq \delta_b \end{cases} \qquad \textbf{(3.20)}$$

in which δ_b is the boundary near bed from which particles are bounced, and h is the surface boundary, y is the initial particle position, y_2 is the final particle position, w_s is the fall velocity and Δt is the timespan of the random walk step. Model will be using a tuning parameter for the fall distance expressed as $w_s\,\Delta t$ to get closer results to the experiments, to cover any energy losses etc (see Eq. 3.13). The bouncing back algorithm is demonstrated in Figure 3.7. Red paths in this figure correspond to the paths due to fall velocity.

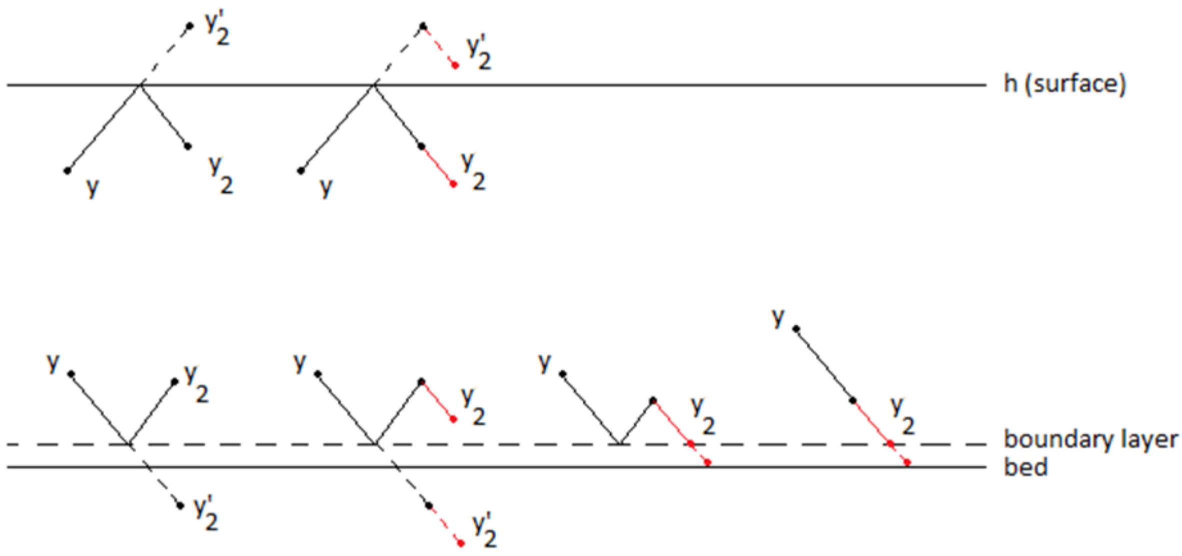

Figure 3.7 : Particle bounce conditions.

3.3 Model Runs

3.3.1 Test matrix

The model will be tested for naturally buoyant particles over smooth bed, for various Re_f values from 500 to 50000. Next, the model will be run for dispersion coefficients for heavy particles such as β = 0.1, 0.2, to 0.9, 1 and 1,5 over smooth bed ($k_s^+ < 5$). Finally, runs for k_s^+ roughness values from 5 to 2000 will be made for β = 0.1, 0.2, to 0.9 and 1. The results will be compared to the previous numerical and analytical studies, such as Sumer (1973, 1974), Elder (1959) and Sayre (1968). All the model equations and algorithms used are summarised in Table 3.1. Also the flow chart of the model is given in Figure 3.8.

3.4. Model equations and parameters

Table 3.1 : Model Parmeters.

Mean Velocity	Van Driest Profile with Cebeci Chang coordinate shift with corrected wake function (Coleman and Alanso, 1983)	$\frac{\bar{u}}{U_f} = \int_0^{y^+} \frac{2dy^+}{1 + \left\{1 + 4\kappa^2(y^+ + \Delta y^+)^2 \left[1 + exp\left(-\frac{(y^+ + \Delta y^+)}{A_d}\right)\right]^2\right\}^{\frac{1}{2}}} + \left(\frac{y^+}{h^+}\right)^2 \left(1 - \frac{y^+}{h^+}\right) + \left(\frac{2\Pi}{\kappa}\right)\left(\frac{y^+}{h^+}\right)^2 \left[3 - 2\frac{y^+}{h^+}\right]$
Turbulence Velocity	Modified Nezu – Nakagawa	$\frac{\sqrt{\overline{v'^2}}}{U_f} = 1.27\, exp\left[-\left(\frac{y}{h} + \frac{\Delta y^+}{Re_f}\right)\right]\left[1 - exp\left(\frac{-(y^+ + \Delta y^+)}{16}\right)\right]$
Roughness Parameter	Cebeci-Chang coordinate shift	$\Delta y^+ = 0.9\left[\sqrt{{k_s}^+} - {k_s}^+ \exp\left(-\frac{{k_s}^+}{6}\right)\right]$; $5 < {k_s}^+ < 2000$
Penetration Length Scale	A Tangent-hyperbolic smoothing	$l_p = 0.21\left(\tanh\left(\left(\frac{y/h}{0.25}\right)^3\right)\right)^{1/3}$
Boundary conditions	A piecewise function, governing the bouncing cases (Kirca 2013)	$y_2 = \begin{cases} y + \Delta y, & \delta_b < y + \Delta y < h \\ 2h - y + \Delta y, & y + \Delta y \geq h \\ max\{\delta_b, [2\delta_b - (y + \Delta y) - 2w_s \Delta t]\}, & y + \Delta y \leq \delta_b \end{cases}$
Settling Velocity	Non-dimentional settling velocity (Rouse parameter)	$\beta = \frac{w}{\kappa U_f}$

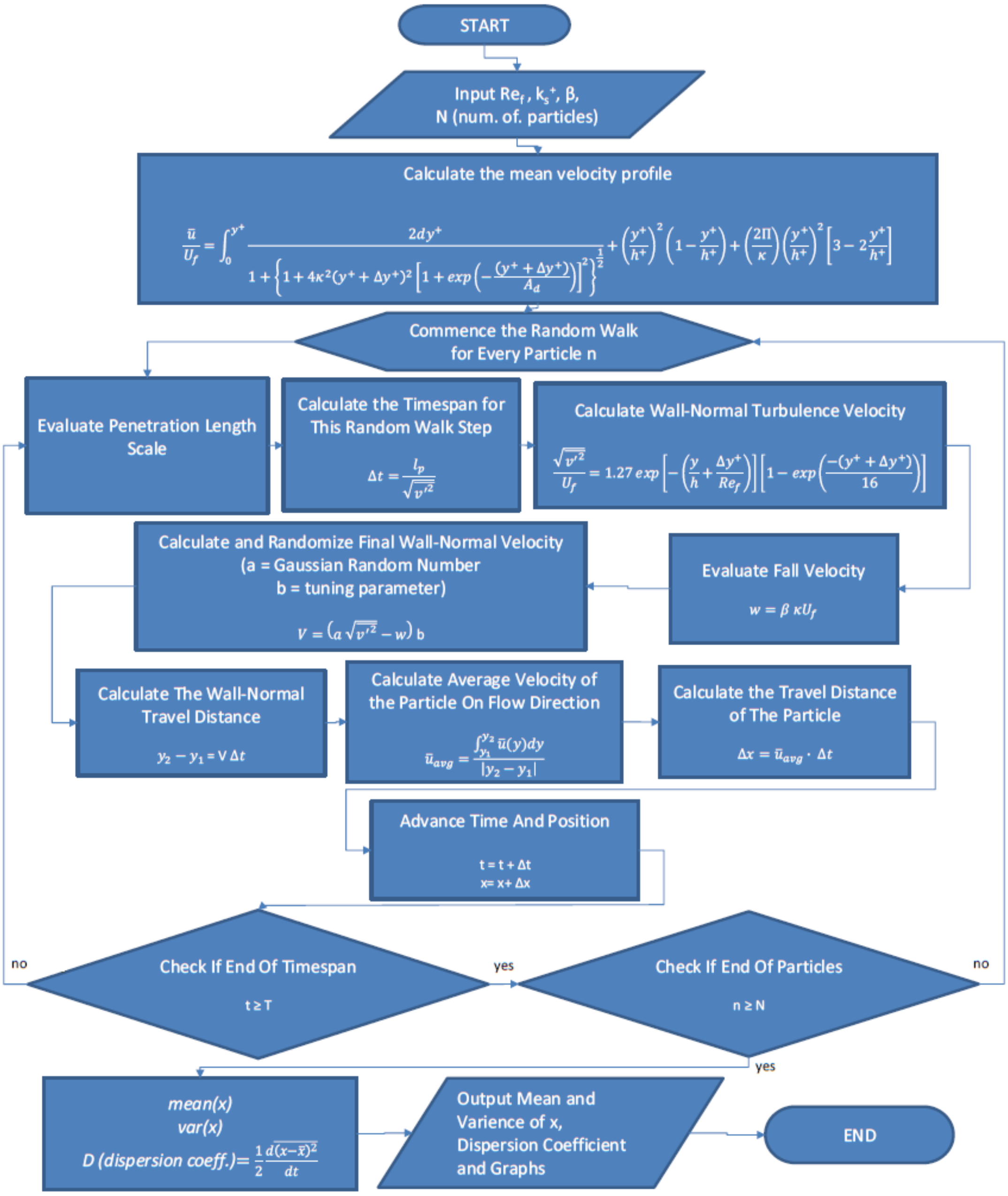

Figure 3.8 Model flow chart.

4. RESULTS

Note that all the variables used in the present model are used as nondimensional quantities. Velocity quantities are made nondimensional upon dividing by U_f (friction velocity), distance quantities are made nondimensional after dividing by h (depth of the flow) and time quantities are made so with dividing with U_f / h. Concentration refers to p.d.f. of the particles. In other words; the spatial sum of concentration over the entire domain would give 1. Nondimentional variables are shown with capital letters. It should also be re-note that the flow domain corresponds to a 2D free surface flow (i.e. a very wide free surface flow). The nondimensional parameters are shown in Equations 4.1 to 4.6

$$T = \frac{tU_f}{h} \tag{4.1}$$

$$Y = \frac{y}{h} \tag{4.2}$$

$$X = \frac{x}{h} \tag{4.3}$$

$$L = \frac{l}{h} \tag{4.4}$$

$$V = \frac{v}{U_f} \tag{4.5}$$

$$U = \frac{\bar{u}}{U_f} \tag{4.6}$$

The model was coded and executed via Matlab©. It was also coded in PHP, for the sake of better accessibility for those who are interested, or need to run different variations; but was not satisfactory in terms of performance. Still, the source code for both languages are ready to be provided by the author on demand.

4.1 Sensitivity Analysis

For the random walk model to give accurate and reliable results, it has to be run with sufficient number of particles. It's obvious that, more the number of particles, more the sensitivity will be, since the simulation results are essentially the statistical characteristics of positions of these N particles. However; achieving a feasible run time for the model is also important. To determine optimum number of points; initially, the model is run for T=20 and the mean and variance of X distance is acquired for different number of particles (Figure 4.1).

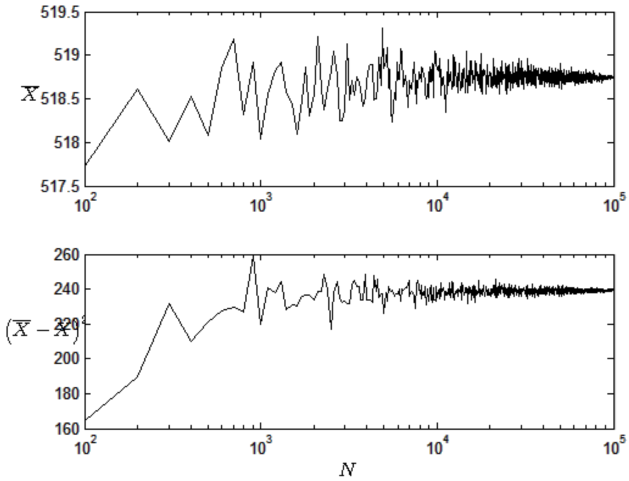

Figure 4.1 : The mean and variance of X for different number of particles.

Seems that with 5000 particles and more, results show that the statistical moments of X demonstrate sufficiently stable characteristics. Therefore, N=5000 particles will be taken as optimum, and model will be run with this many of particles. Note that this sensibility variable can easily be increased according to the computer's power.

4.2 Neutrally Buoyant Particles on Smooth Wall

For smooth wall and neutrally buoyant particles, there is Elder's (1959) (and later Sumer 1974) analytical results, as well as Sumer (1973) numerical results. They can be seen along the present model results in Table 4.1, and Figure 4.2.

Table 4.1 : Results for neutrally buoyant particles over smooth wall.

Re_f	D/hU$_f$		
	Elder 1959 and Sumer 1974 analytical solution	**Sumer 1973 Numerical**	**Present Model**
500	5,93	-	5.89
800		6.5	-
1000		8.45	5.59
5000		-	6.61
10000		-	5.86
20000		-	6.67
50000		-	5.55
100000		-	6.27
500000		-	6.04

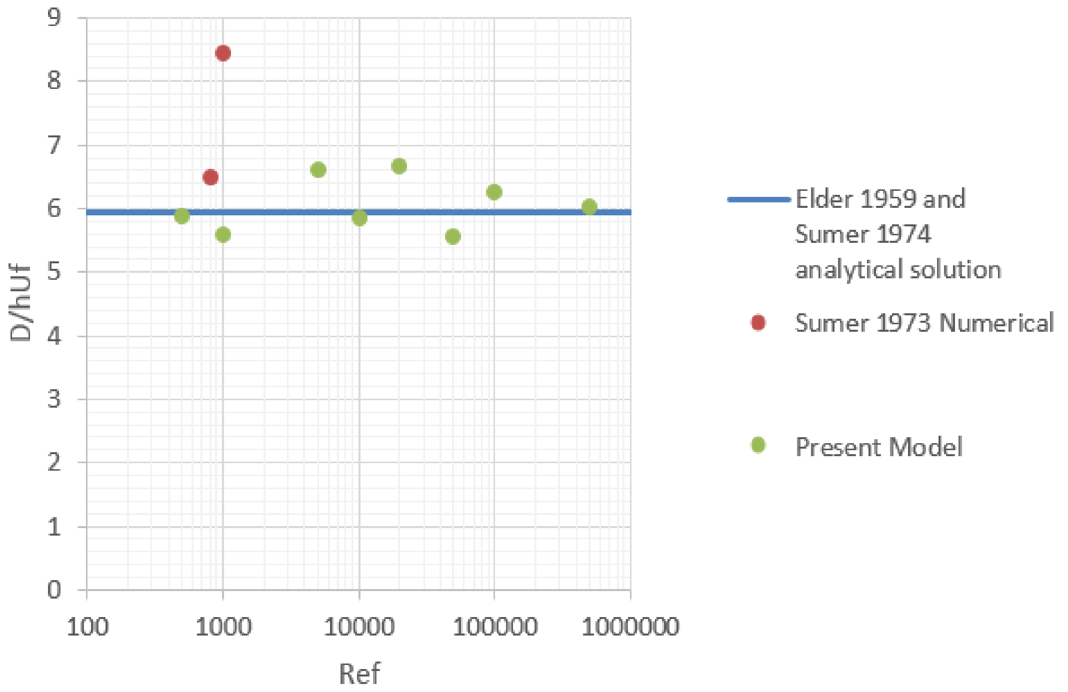

Figure 4.2 : Results for neutrally buoyant particles over smooth wall.

As seen, the Friction Reynolds Number has no significant effect on results, as suggested by the analytical solutions (note that the horizontal scale of Figure 4.1 is logarithmic). We will be working with Friction Reynolds Number of 10000 for the heavy particles and rough bed. This Reynolds number roughly corresponds to the scale of geophysical flows such as marine currents, estuarine and riverine flow.

4.3 Heavy Particles on Smooth Wall

For heavy particles on smooth wall, we also have previous results from Sumer's (1974) analytical, and Sayre's (1968) numerical solutions. All can be seen along the results from the present model in Table 4.2. and Figure 4.3.

Table 4.2 : Results for heavy particles on smooth wall.

β	**D(β) / D₀**		
	Sumer (1974)	**Sayre (1968)**	**Present Model**
0	1.00	1.00	1.00
0.1	1.23	1.11	1.38
0.2	1.52	1.21	1.69
0.3	1.90	1.28	2.47
0.4	2.42		3.19
0.5	3.15		4.38
0.6	4.16		6.19
0.7			7.25
0.8			7.90
0.9			7.26
1			4.81
1.5			4.82

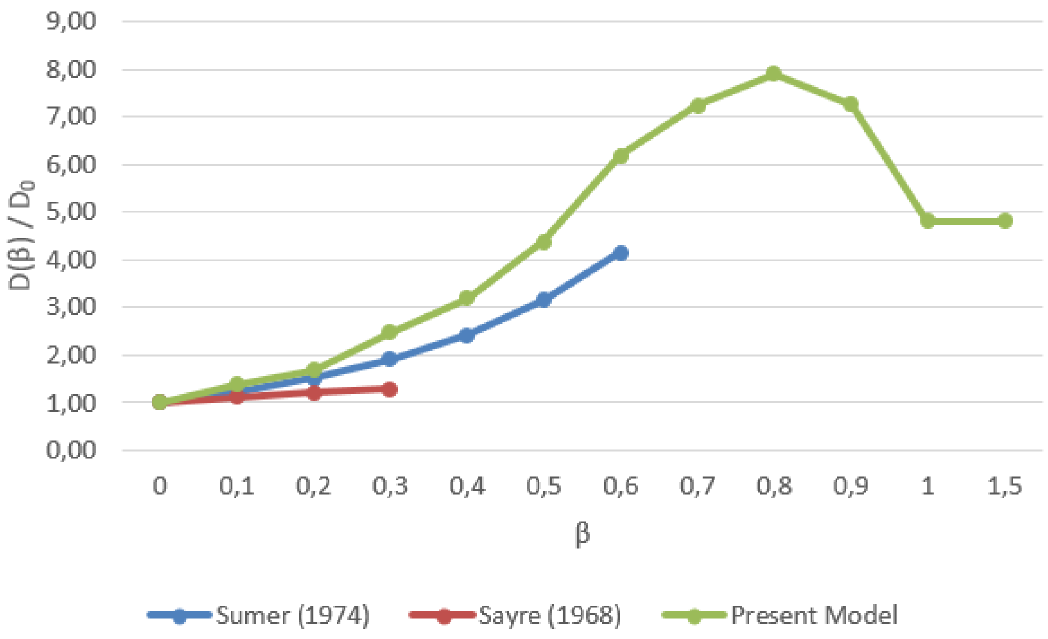

Figure 4.3 : Results for heavy particles on smooth wall.

As the fall velocity increases, the particles spend more time close to the bed where the velocity gradient and wall-normal turbulence is stronger. Therefore, the dispersion coefficient gets larger as the particles get heavier. Note that, as the settling velocities of the particles increase after a certain point (β=1), they tend to settle early and mostly are carried as bedload or or in contact with bed with closer velocities near the bottom layer. This presumably causes the decrease in the dispersion coefficient. For heavy particles, concenration profile comparison with Sumer (1974) is shown in the Figures 4.4 to 4.9. In those figures, C_0 is the concentration moment (i.e. the vertical variation of p.d.f. of particles) and blue curves corresponds to the concentration profiles calculated via the Aris concentration moments (Sumer, 1974). As can be seen, as the settling velocity increases the particle concentration near the bed tends to increase while the nearbed concentration decreases. The concentration profile would give unity for a neutrally buoyant particle.

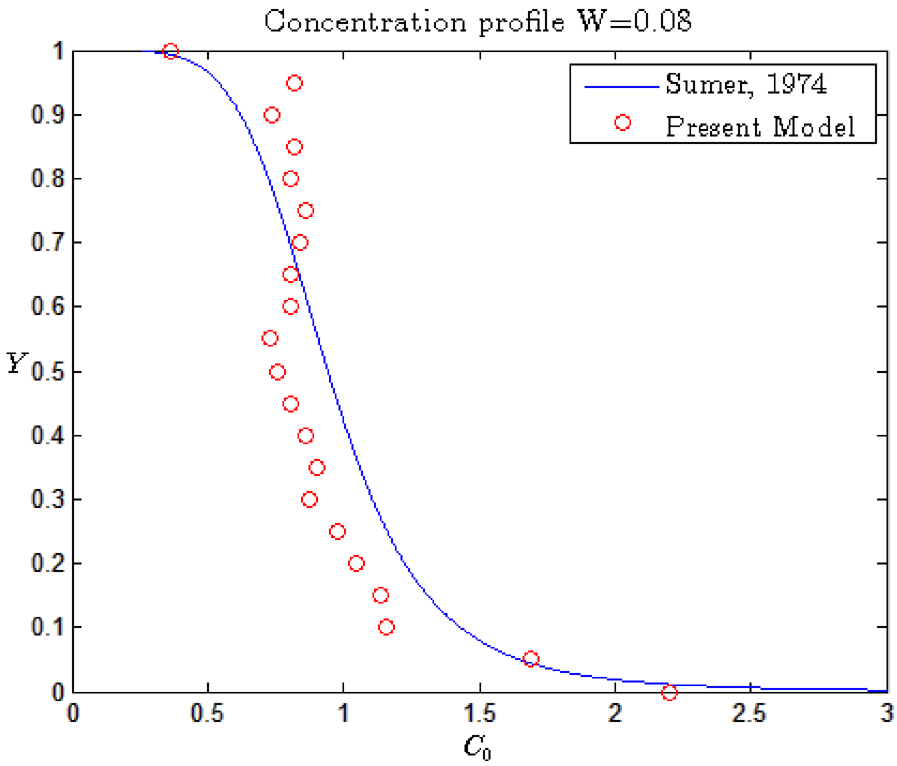

Figure 4.4 : Concentration profile for β = 0.2.

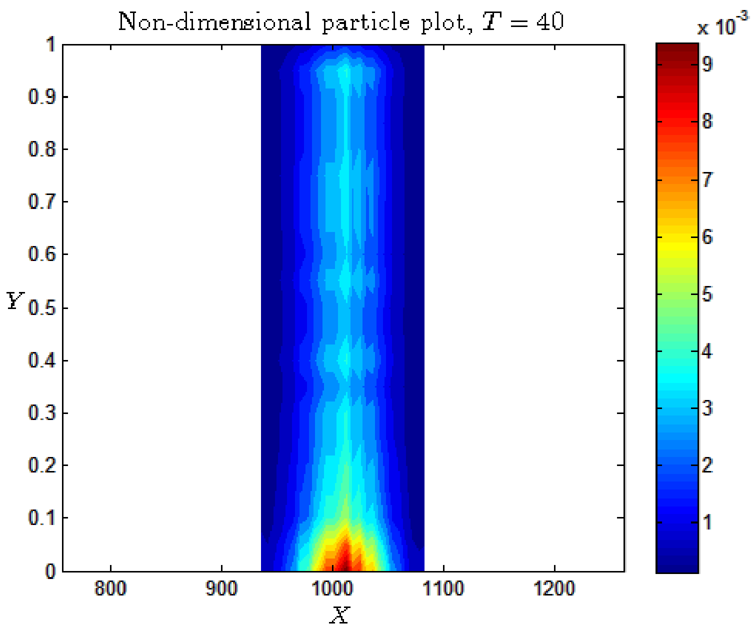

Figure 4.5 : Final particle concentrations for β = 0.2.

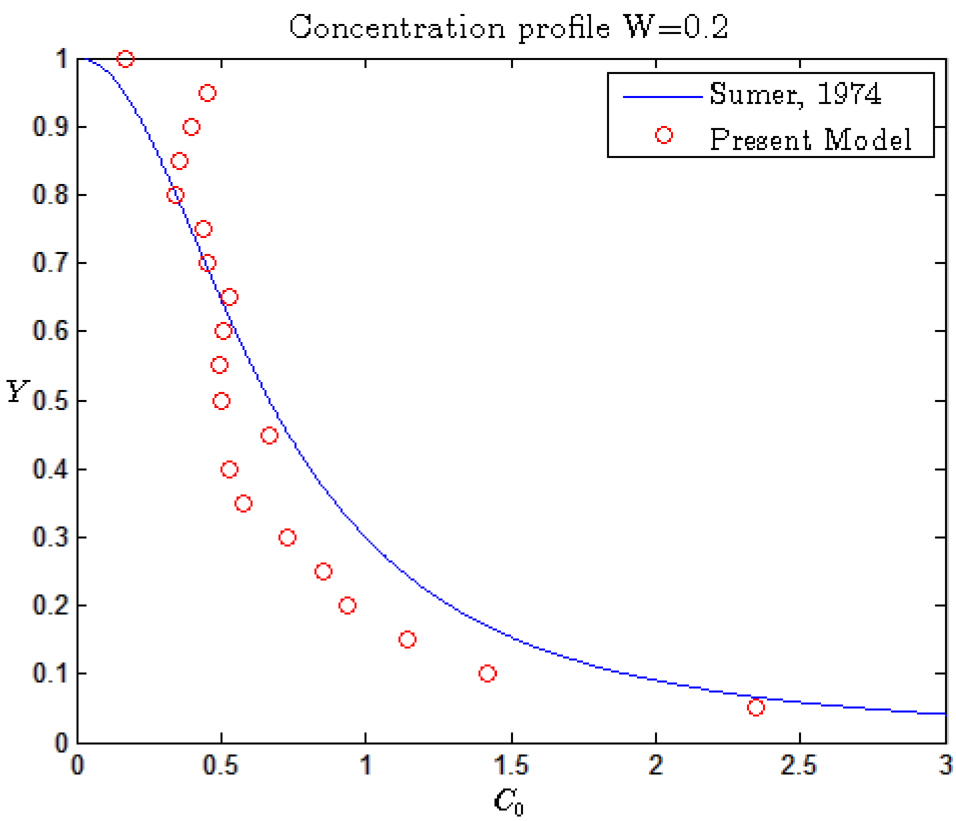

Figure 4.6 : Concentration profile for β = 0.5.

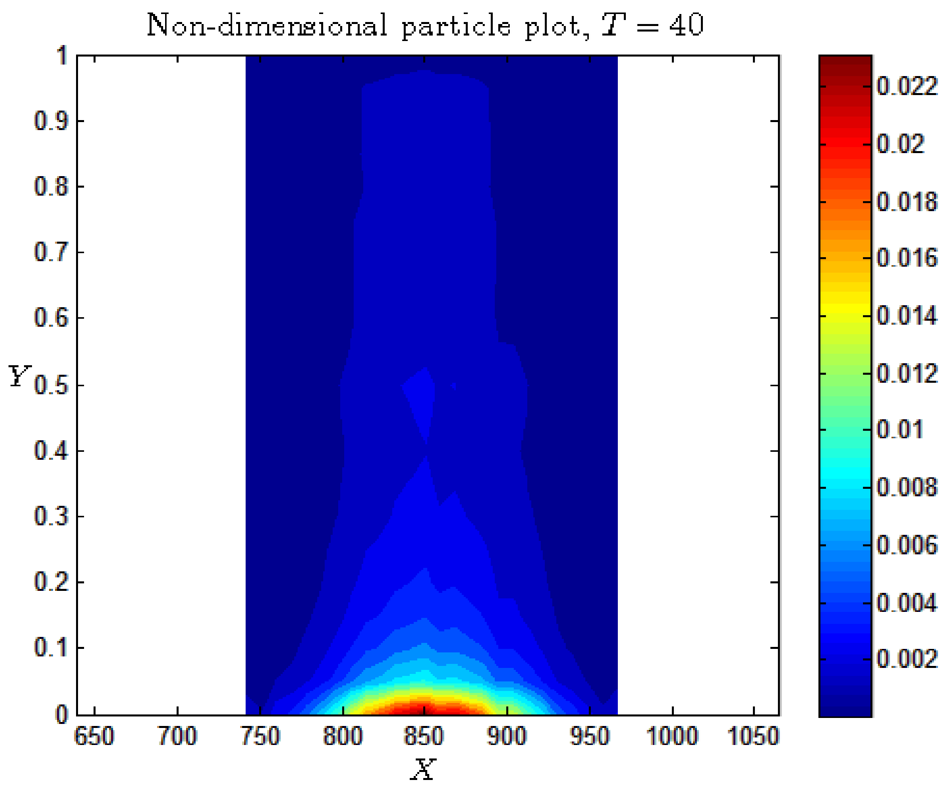

Figure 4.7 : Final particle concentrations For β = 0.5

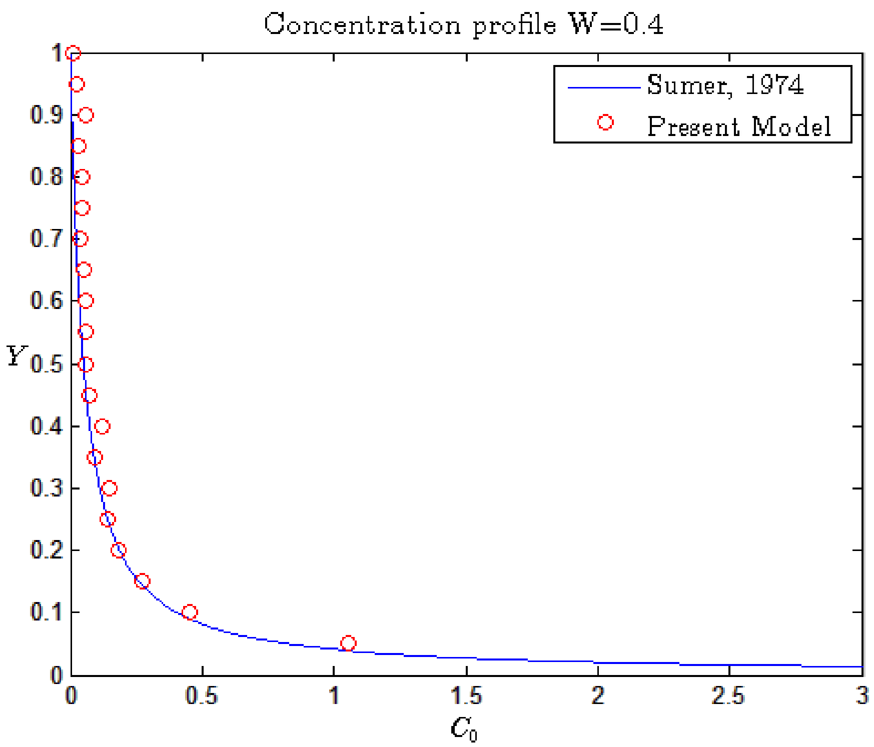

Figure 4.8 : Concentration profile for β = 1

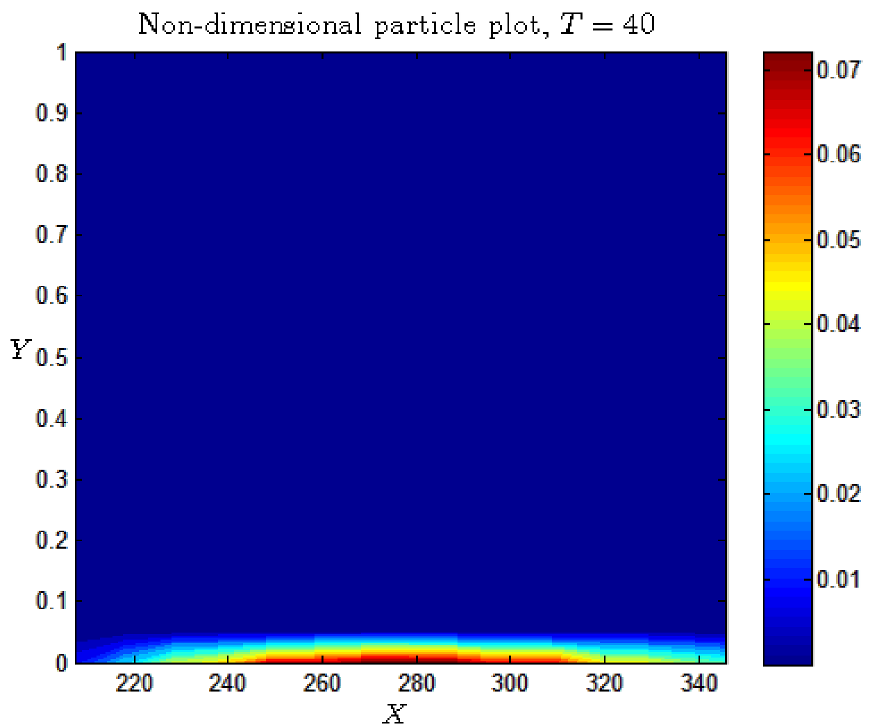

Figure 4.9 : Final particle concentrations for β = 1.

4.4 Neutrally Buoyant Particles on Rough Wall

The present model is designed to inspect the effect of bed roughness on dispersion. While there is no previous data to compare for this inspection, results from the present model are as in Table 4.3 and Figure 4.10.

Table 4.3 : Dispersion coefficients for different roughness values with Re_f = 10000

K_s^+	Ks/h	D/hU_f	Wall Category
10	0.001	6.24	Transitionally rough wall
20	0.002	6.66	
50	0.005	6.19	
100	0.010	6.42	Fully rough wall
200	0.020	6.18	
500	0.050	6.21	
1000	0.100	6.06	
1500	0.150	6.08	
2000	0.200	5.86	

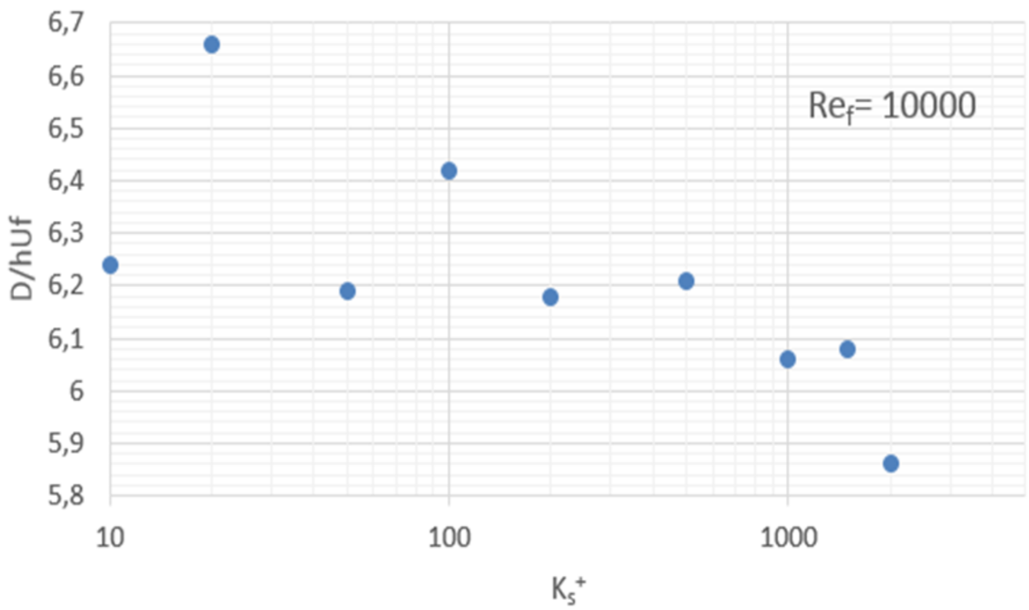

Figure 4.10. : Dispersion coefficients for different roughness values with Re_f = 10000.

As seen in the results, with the same Friction Reynolds Number, dispersion coefficient tends to decrease as roughness increases. However, it is observed that roughness has no significant effect on concentration profiles unless it becomes so large (i.e. the roughness elements penetrate deep into the flow domain).

Previously, it was inspected if the dispersion coefficient varies according to the friction Reynolds Number, and concluded that it did not have any significant effect. Now the model is run for different friction Reynolds Numbers on rough bed and results are given in Table 4.4 and Figure 4.11 for $k_s^+ = 100$.

Table 4.4 : Dispersion coefficients for different Reynolds Numbers on rough bed

Re_f	Ks/h	D/hU_f
500	0.2000	5.4
1000	0.1000	6.34
5000	0.0200	6.17
10000	0.0100	6.42
20000	0.0050	5.62
50000	0.0020	5.81
100000	0.0010	6.05
500000	0.0002	6.03

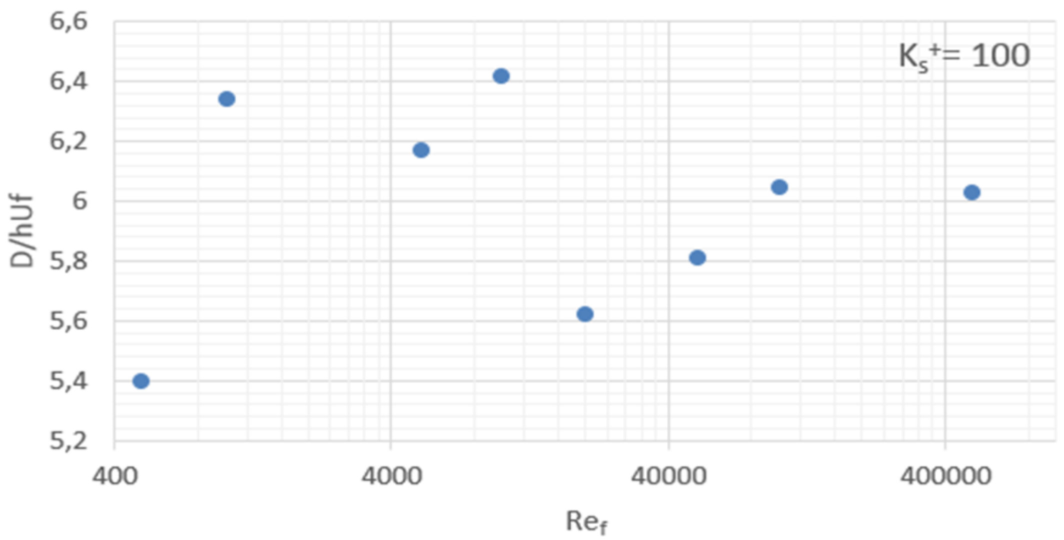

Figure 4.11 : Dispersion coefficients for different Reynolds Numbers on rough bed $k_s^+ = 100$.

Results show that, again on rough bed, Friction Reynolds Number has no significant effect on dispersion coefficient unless it becomes so large (i.e. the roughness elements penetrate deep into the flow domain). In Figure 4.12, dispersion coefficient values according to relative roughness can be seen. Results show that with increasing relative roughness, dispersion coefficient tends to slightly decrease.

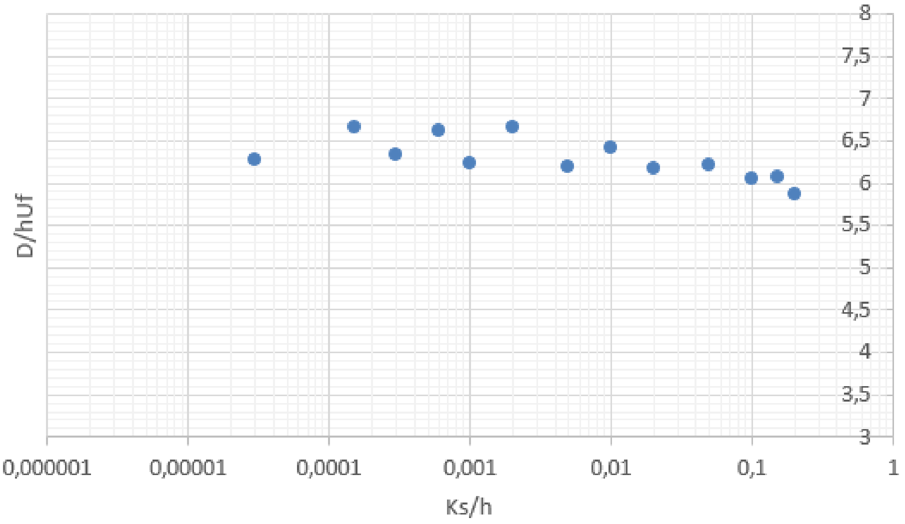

Figure 4.12 : Dispersion coefficient with relative roughness (k_s / h).

4.5 Heavy Particles on Rough Wall

Lastly, the model is run for particles with different settling velocities, on walls with different roughnesses. The results are shown in Table 4.5, Figure 4.13 and 4.14.

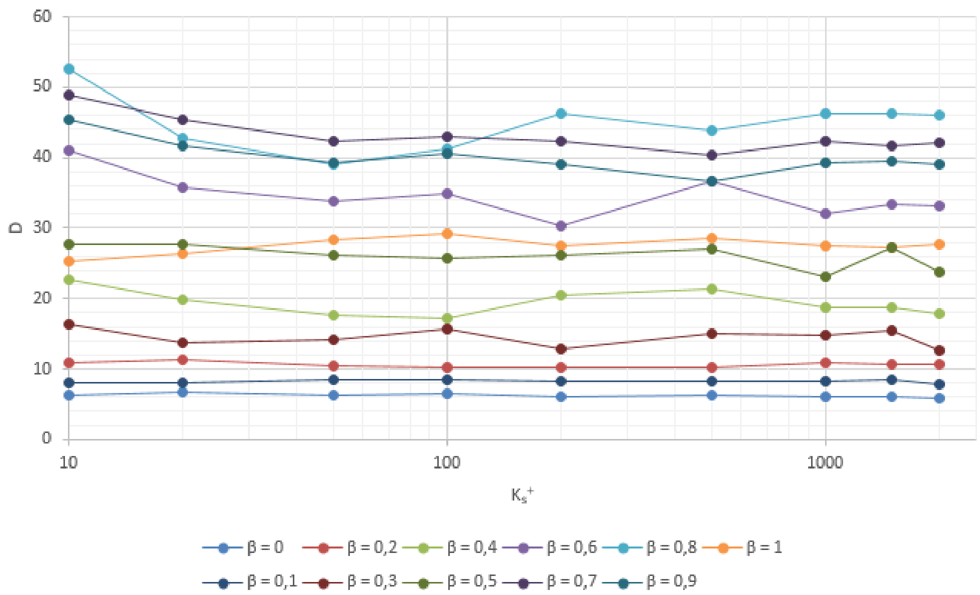

Figure 4.13 : Dispersion coefficients for particles with settling velocities on rough wall.

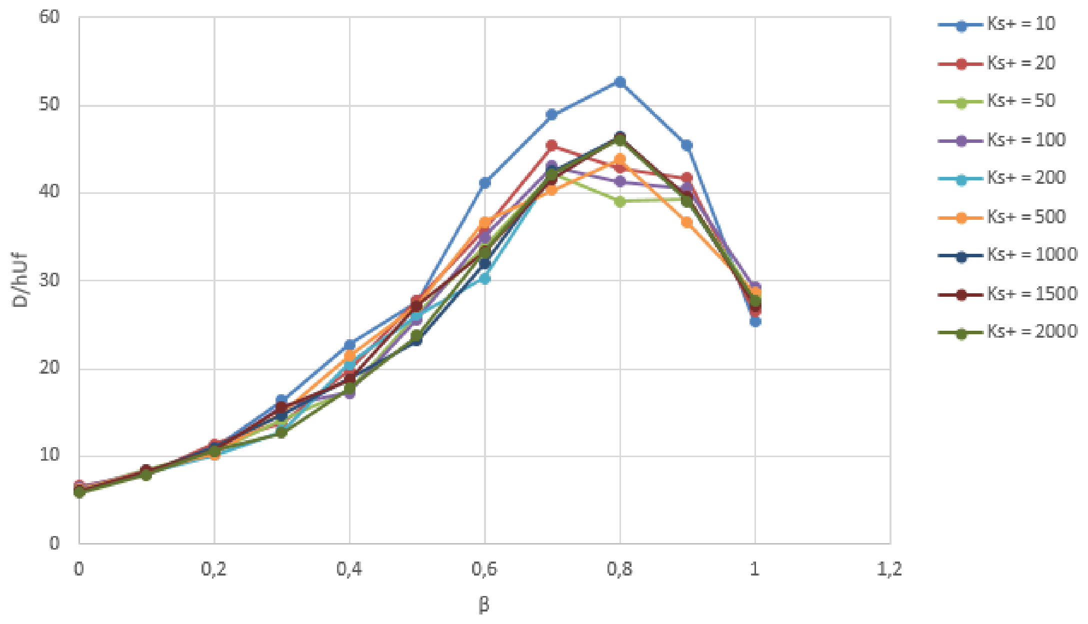

Figure 4.14 : D / hU_f for different bed roughnesses for settling velocities.

Results indicate the effect of bed roughness to decrease with increasing particle fall velocity.

Table 4.5. : Particles with settling velocities on rough wall.

K_s^+	**B**										
	0	**0.1**	**0.2**	**0.3**	**0.4**	**0.5**	**0.6**	**0.7**	**0.8**	**0.9**	**1**
10	6.24	8.12	10.91	16.33	22.73	27.70	41.11	48.89	52.64	45.35	25.35
20	6.66	8,00	11.42	13.75	19.82	27.80	35.70	45.38	42.88	41.71	26.50
50	6.19	8.48	10.54	14.14	17.55	26.18	33.77	42.30	39.03	39.28	28.28
100	6.42	8.39	10.33	15.66	17.27	25.66	34.93	43,00	41.29	40.53	29.17
200	6.18	8.17	10.18	12.88	20.60	26.13	30.29	42.31	46.30	39.10	27.57
500	6.21	8.31	10.23	14.98	21.38	27.15	36.74	40.27	43.80	36.64	28.64
1000	6.06	8.17	10.97	14.72	18.81	23.20	31.98	42.41	46.35	39.24	27.57
1500	6.08	8.38	10.65	15.55	18.72	27.21	33.28	41.62	46.30	39.50	27.20
2000	5.86	7.89	10.61	12.70	17.77	23.79	33.20	42.13	46.10	39.01	27.78

4.6 Remark On A Practical Application

In this subsection, a numerical example is given as to how the present model can be used in practical applications.

Consider a river with h = 1m depth and q = 0,8 m^3/s/m flow. Friction velocity U_f is measured approximately 2,5 cm/s for this river. Soil from a nearby excavation was mixed with the flow with the diameter of D_{50} = 0,08 mm (i.e. silt). Find the dispersion coefficient for the soil if;

a) Nondimensional Nikuradse equivalent sand roughness of the river bed is $k_s^+ = 3$
b) Nondimensional Nikuradse equivalent sand roughness of the river bed is $k_s^+ = 2000$
Solution is as follows:
Settling velocity is determined from Figure 4.15.

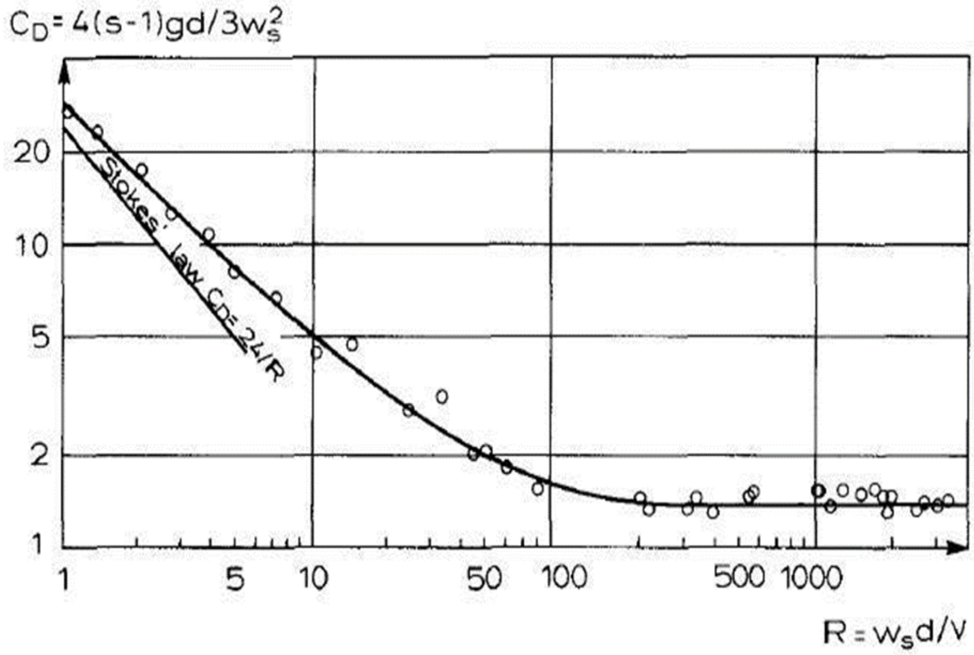

Figure 4.15 : C_D according to Re (Kirca, 2013b).

Density of the soil is 1,5 g/cm^3

Table 4.6 : Settling velocity guess.

Guessed Settling Velocity - w_s (m/s)	$Re = \frac{w_s D}{\upsilon}$	$C_D = \begin{cases} \frac{24}{Re}, & Re < 1 \\ Fig.5.1, & Re \geq 1 \end{cases}$	$C_D = \frac{4\left(\frac{\gamma_s}{\gamma} - 1\right) gD}{3{w_s}^2}$	Result
0.01	0.8	30	5.22	Too high
0.005	0.4	60	20.91	Too high
0.002	0.16	150	130.67	Little high
0.0018	0.144	166.67	161.3	Correct

$$W = \frac{w_s}{U_f} = \frac{0.0018}{0.025} = 0.072 \quad \textbf{(4.7)}$$

$$\beta = \frac{W}{\kappa} = \frac{0.072}{0.4} = 0.18 \quad \textbf{(4.8)}$$

$$Re_f = \frac{hU_f}{\upsilon} = \frac{1 * 0.025}{10^{-6}} = 25000 \quad \textbf{(4.9)}$$

If the model is run for $\boldsymbol{Re_f = 25000}$, $\boldsymbol{\beta = 0.18}$ and $\boldsymbol{{k_s}^+ = 3}$, the dispersion coefficient will be 10.66

And if it is run for $\boldsymbol{Re_f = 25000}$, $\boldsymbol{\beta = 0.18}$ and $\boldsymbol{{k_s}^+ = 2000}$, the dispersion coefficient will be 10.23, %4 lower.

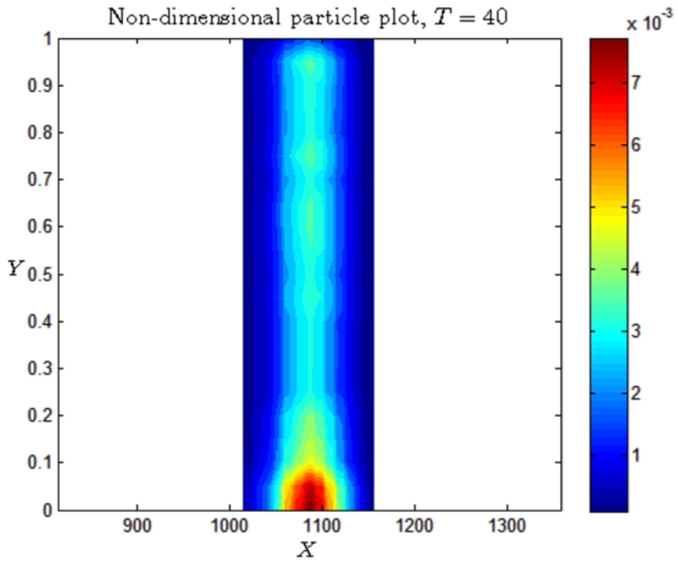

Figure 4.16 : Soil concentration for $k_s^+ = 3$ at T = 40.

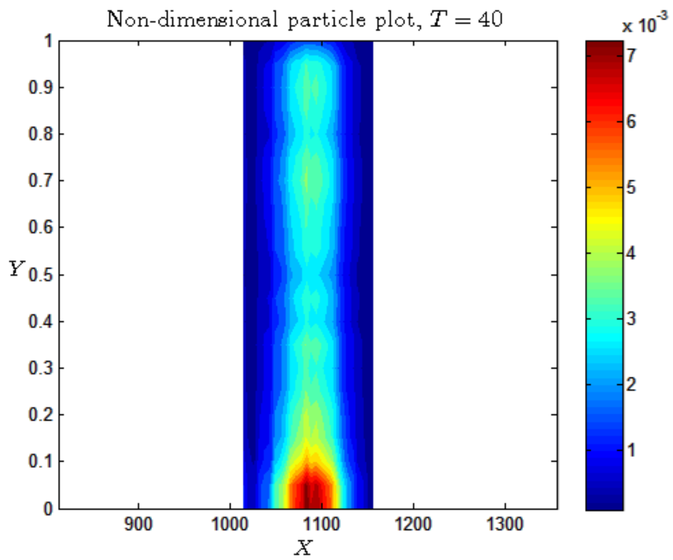

Figure 4.17 : Soil concentration for $k_s^+ = 2000$ at T = 40.

5. CONCLUSION

To wrap up the whole concept, the software model built with the parameters mentioned in the method section, seems to provide results that agree quite well with the previous studies both numerical and analytical.

For neutrally buoyant particles on smooth bed, the model result around 6 seems to sufficiently agree with the analytical solution of Sumer (1974) and Elder (1959), while the results for heavy particles over smooth bed have the same tendency with the same study of Sumer (1974). Additionally, as the settling velocity of the particles increase, the dispersion coefficient tends to decrease as expected, as the particles begin to lose their buoyancy and transported more and more close to the bed where the velocity gradient and turbulence is larger. And after Rouse parameter $\beta = 0{,}8 - 1$, they seem to be transported as bedload or in contact with bed all along. This is somehow expected since it is well-known that the suspension regime tends to be terminated for $\beta \approx 1$, in harmony with our present results.

As for the innovative part of this study, Cebeci-Chang coordinate shift was included in the model along with the Coleman and Alanso wake function correction to have a refined profile and be able to inspect the effect of bed roughness on the dispersion of the heavy particles. Results show that, for neutrally buoyant particles, as roughness increases, dispersion coefficient tends to slightly decrease, especially when the roughness elements penetrates deeper into the flow domain (i.e. for high ks/h values). As the settling velocity of the particles increase, however, the effect of roughness on the dispersion seems to fade.

Applying on a practical situation, the model has given similar results, and shown a slight decrease in the dispersion coefficient with increased bed roughness. A more refined result would have been given if the model had run with more particles, according to the ability of the computer used.

Fine-tuning and improving on numerical models has no end. For the present one, refined and improved versions of previous methods were used, with the performance provided by a modern 4 core computer. Effects of roughness have also been modelled numerically for the first time. If the number of particles released for random walk modelling had been higher, the precision of the results could have been increased. Applying the algorithm in this study, future research can be implemented to modify the present results.

Value and importance of numerical modelling lies on its practical use. A good interface will make it possible for the end-users to get the results they need without much effort, which makes it an important tool. But regardless of how powerful tools there are, they have no value if not used. Turbulent dispersion studies have a very important role in pollution control, sediment transport, biochemical assessment lifecycle analysis and environmental impact assessments. The present model is hoped to be useful for the prediction of the magnitude of pollutions caused by dispersing pollutant material inside marine, atmospheric and fluvial boundary layers. A useful application of the present model would be the dredging operations conducted in marine environment, in which fine sediments are dispersed and causes excess turbidity and hazard to biota.

REFERENCES

Bachelor, G. K. (1965). The motion of small particles in turbulent flow. *2^{nd} Australian Conf. on Hydraulic And Fluid Mech. No:19, University of Auckland, New Zealand.*

Bayazıt, M. (1972). Random Walk Model For Motion Of A Solid Particle In Turbulent Open-Channel Flow. *J. Fluid Mech., vol. 10, p.1-14*

Beer, T., **Young, P. C.** (1983). Longitudinal dispersion in natural streams. *J. Environ. Eng. Vol. 109, p.1049.*

Bencala, K.E., Walters, R.A., (1983). Simulation of solute transport in a mountain pool and-riffle stream: a transient storage model. *Water Resources Research 19 (3), 718–724.*

Brown, G. L and Roshko, A. (1974). On density effect and large structure in the turbulent mixing layers. *J. Fluid Mech., vol. 64, p.775*

Cebeci, T. and Chang, K.C. (1978). Calculation of incompressible rough-wall boundary-layer flows. *AIAA Journal, vol. 16, No. 7, p.730.*

Coleman, N. L. and Alanso, C.V. (1983). Two-Dimensional channel flows over rough surfaces. *J. Hydraul. Eng., Proc. ASCE, vol 109,No. 2, p.175.*

Deng, Z. Q., Singh, V. P., & Bengtsson, L. (2001). Longitudinal dispersion coefficient in single channel streams. *Journal of Hydraulic Engineering, 128(10), 901–916.*

Deng, Z. Q., and Jung, H. S. (2008). Scaling dispersion model for pollutant transport in rivers. *Department of Civil and Environmental Engineering, Louisiana State University, LA.*

Elder, J. (1959). The dispersion of marked fluid in turbulent shear flow. *J. Fluid Mech., vol. 5, p. 544.*

Fischer, H. B. (1967). The mechanics of dispersion in natural streams. *Journal of Hydraulic Division, American Socitey of Civil Engineering, 93(6), 187–216*

Fischer, H. B., List E. J., Koh, R. C. Y, Imberger, J., Brooks, N. H. (1979). Mixing in inland and coastal waters. *Academic Press Inc. London.*

Grass, A. J. (1971). Structural features of turbulent flow over smooth and rough boundaries. *J. Fluid Mech., vol. 50, p.233.*

Harvey, J.W., Wagner, B.J., Bencala, K.E. (1996). Evaluating the reliability of the stream tracer approach to characterize stream–subsurface water exchange. *Water Resources Research 32 (8), 2441–2451.*

Iwasa, Y., and Aya, S. (1991). Predicting longitudinal dispersion coefficient in openchannel flows. *In Proceedings of international symposium on environmental hydraulics, Hong Kong, (pp. 505–510).*

Kashefipur, S. M., & Falconer, A. (2002). Longitudinal dispersion coefficients in natural channels. *In Proceedings of the fifth international hydro informatics conference, 1–5 July, Cardiff University. (pp. 95–102).*

Kim, J. (1987). Evolution of a vertical structure associated with the bursting event in channel flow. *Turbulent Shear Flows 5. Springer-Verlag, pp. 221.*

Kirca, V. S. O. (2013a). Dispersion in wave boundary layers. *Mermaid project presentation. Santander, Denmark*

Kirca, V. S. O. (2013b). Lecture notes on Water Supply Management. *Beykent University, Istanbul.*

Kline S.J., Reynolds. W. C., Schraub, F. A., Runstadler, P. W. (1967). The structure of turbulent boundary layers. *J. Fluid Mech., vol. 30, p.741.*

Kolmogorov, A. N. (1941). The local structure of turbulence in incompressible viscous fluid for very large Reynolds numbers. *Proc. R. Soc. Lond. A.*

Koussis, A. D., & Rodriguez-Mirasol, J. (1998). Hydraulic estimation of dispersion coefficient for streams. *Journal of Hydraulic Engineering, ASCE, 124, 317–320.*

Li, Z. H., Huang, J., & Li, J. (1998). Preliminary study on longitudinal dispersion coefficient for the gorges reservoir. *In Proceedings of the seventh international symposium environmental hydraulics, 16–18 December, Hong Kong, China.*

Liu, H. (1977). Predicting dispersion coefficient of stream. *Journal of Environment Engineering Division, ASCE, 103(1), 59–69.*

McQuivey, R. S., & Keefer, T. N. (1974). Simple method for predicting dispersion in streams. *Journal of Environmental Engineering Division, American Society of Civil Engineering, 100(4), 997–1011.*

Moin, P., Kim, J. (1982). Numerical investigation of turbulent channel flow. *J. Fluid Mech., vol. 118, p.341.*

Nezu, I. and Nakagawa, H. (1993). Turbulence in free surface flows. *A. A. Balkema, Rotterdam.*

Nordin, C.F., Troutman, B.M., (1980). Longitudinal dispersion in rivers: the persistence of skewness in observed data. *Water Resources Research 16 (1), 123–128.*

Riahi-Madvar, H., Ayyoubzadeh, S. A., Khandangi, E., Ebadzadeh, M. M. (2008). An expert system for predicting longitudinal dispersion coefficient in natural streams by using ANFIS. *Department of Water Structures Engineering, Tarbiat Modares University, Department of Computer Engineering, Amirkabir University of Technology, Tehran.*

Runkel, R.L. (1998). One-Dimensional Transport with Inflow and Storage (OTIS): a Solute Transport Model for Streams and Rivers. *Water Resources Investigations Report 98-4018. U.S. Geological Survey, Denver.*

Sayre, W. W. (1968). *Hydraulic Papers, No. 3, Colorado State University, Fort Collins.*

Schmid, B.H. (1995). On the transient storage equations for longitudinal solute transport in open channels: temporal moments accounting for the first-order decay. *Journal of Hydraulic Research 33 (5), 595–610.*

Seo, I. W., & Cheong, T. S. (1998). Predicting longitudinal dispersion coefficient in natural Stream. *Journal of Hydraulic Engineering, 124(1), 25–32.*

Sumer, B. M. (1973). Simulation of dispersion of suspended particles. *Journal of the Hyrdolics Division. Vol. 99, No. 10 pp. 1705-1726*

Sumer, B. M. (1974). Mean velocity and longitudinal dispersion of heavy particles in turbulent open-channel flow. *J. Fluid Mech. Vol. 65, Issue 01, pp 11-28.*

Sumer, B. M. (2007). Lecture notes on turbulence. *Technical University of Denmark.*

Winant, C. D., Browand, F. K. (1974). Vortex pairing: the mechanism of turbulent mixing layer growth at moderate Reynolds Number. *J. Fluid Mech., vol. 63, pp. 237-255*

Yip, M. K. (2012). Science of soccer lecture notes. *University of Hong Kong.*

Url-1 < *http://en.wikipedia.org/wiki/Anemometer*>, date retrieved 01.05.2015.

CURRICULUM VITAE

Name Surname **: Selçuk DEMİRBAŞ**

Place and Date of Birth **: Istanbul / 02.12.1984**

E-Mail **: selcukdemirbas@gmail.com**

EDUCATION:

B.Sc. **: Civil Engineering / Yıldız Technical University**

PROFESSIONAL EXPERIENCE AND REWARDS:

- İKY İnşaat A.Ş. – Chief Technical Officer, 2014 – cont.
- Demirbaş Mühendislik Ltd. – Manager, 2013 – 2014
- Başakkent İnşaat A.Ş. – Technical Manager, 2011 – 2013
- EDOK Muh. Hizm. Dest. Eğt. K.lığı – Const. Planning Officer, 2010 – 2011
- Karadeniz Elk. Ürt. A.Ş. – Field Engineer, 2008 – 2010
- Demirbaş İnşaat Ltd. – Survelliant, 2004 - 2005